

# Perturbations to the $\mu - \tau$ symmetry, leptogenesis, and lepton flavor violation with the type II seesaw mechanism

Manikanta Borah,<sup>\*</sup> Debasish Borah,<sup>†</sup> and Mrinal Kumar Das<sup>‡</sup>

*Department of Physics, Tezpur University, Tezpur 784028, India*

Sudhanwa Patra<sup>§</sup>

*Center of Excellence in Theoretical and Mathematical Sciences,*

*Siksha O Anusandhan University, Bhubaneswar 751030, India*

(Received 19 August 2014; published 21 November 2014)

We study the possibility of generating nonzero reactor mixing angle  $\theta_{13}$  by perturbing the  $\mu - \tau$  symmetric neutrino mass matrix. The leading-order  $\mu - \tau$  symmetric neutrino mass matrix originates from a type I seesaw mechanism, whereas the perturbations to  $\mu - \tau$  symmetry originate from a type II seesaw term. We consider four different realizations of  $\mu - \tau$  symmetry, bimaximal mixing, tribimaximal mixing, hexagonal mixing, and golden ratio mixing, all giving rise to  $\theta_{13} = 0$ ,  $\theta_{23} = \frac{\pi}{4}$  but different nonzero values of solar mixing angle  $\theta_{12}$ . We assume a minimal  $\mu - \tau$  symmetry breaking type II seesaw mass matrix as a perturbation and calculate the neutrino oscillation parameters as a function of type II seesaw strength. We then consider the origin of nontrivial leptonic  $CP$  phase in the charged lepton sector and calculate the lepton asymmetry arising from the lightest right-handed neutrino decay by incorporating the presence of both type I and type II seesaws. We constrain the type II seesaw strength as well as the leptonic  $CP$  phase (and hence the charged lepton sector) by comparing our results with experimental neutrino oscillation parameters as well as the Planck bound on the baryon-to-photon ratio. Finally, we extend our analysis on lepton flavor violating decays like  $\mu \rightarrow e\gamma$  and  $\mu \rightarrow eee$  due to the exchange of a TeV scale Higgs triplet scalar within the low scale type II seesaw framework. The branching ratios for these lepton flavor processes are examined with the small type II perturbation term  $\omega$ , and the estimated values are very close to the experimental bound coming from current search experiments.

DOI: 10.1103/PhysRevD.90.095020

PACS numbers: 12.60.-i, 12.60.Cn, 14.60.Pq

## I. INTRODUCTION

The standard model (SM) of particle physics has been established as the most successful theory describing all fundamental particles and their interactions except gravity, especially after the discovery of its last missing piece, the Higgs boson in 2012. Despite its huge phenomenological success, the SM fails to explain many observed phenomena in nature. The origin of tiny neutrino mass and matter-antimatter asymmetry are two of such phenomena that can be explained only within the framework of some beyond the standard model (BSM) physics. Neutrinos that remain massless in the SM have been shown to have tiny but nonzero mass (12 orders of magnitude smaller than the electroweak scale) by several neutrino oscillation experiments [1]. Recent neutrino oscillation experiments T2K [2], Double ChooZ [3], Daya-Bay [4], and RENO [5] have not only made the earlier predictions for neutrino parameters more precise but also predicted the nonzero value of the reactor mixing angle  $\theta_{13}$  as shown in Table I. Recent global

fits for different oscillation parameters within their  $3\sigma$  range taken from Refs. [6] and [7] are presented below in Table II.

Several BSM frameworks have been proposed to explain the origin of tiny neutrino mass and the pattern of neutrino mixing. Tiny neutrino mass can be explained by seesaw mechanisms, which broadly fall into three types, type I [8], type II [9], and type III [10], whereas the pattern of neutrino mixing can be understood by incorporating additional flavor symmetries.

The neutrino oscillation data before the discovery of nonzero  $\theta_{13}$  were in perfect agreement with the  $\mu - \tau$  symmetric neutrino mass matrix. Four different neutrino mixing patterns that can originate from such a  $\mu - \tau$  symmetric neutrino mass matrix are bimaximal mixing (BM) [11], tribimaximal mixing (TBM) [12], hexagonal mixing (HM) [13], and golden ratio mixing (GRM) [14]. All these scenarios predict  $\theta_{23} = 45^\circ$ ,  $\theta_{13} = 0$  but different values of solar mixing angle  $\theta_{12} = 45^\circ$  (BM),  $\theta_{12} = 35.3^\circ$  (TBM),  $\theta_{12} = 30^\circ$  (HM), and  $\theta_{12} = 31.71^\circ$  (GRM). However, in view of the fact that the latest experimental data have ruled out  $\sin^2 \theta_{13} = 0$ , one needs to go beyond these  $\mu - \tau$  symmetric frameworks. Since the experimental value of  $\theta_{13}$  is still much smaller than the other two mixing angles,  $\mu - \tau$  symmetry can still be a valid approximation, and the nonzero  $\theta_{13}$  can be accounted for by incorporating

<sup>\*</sup> mani@tezu.ernet.in

<sup>†</sup> dborah@tezu.ernet.in

<sup>‡</sup> mkdas@tezu.ernet.in

<sup>§</sup> sudha.astro@gmail.com

the presence of small perturbations to  $\mu - \tau$  symmetry coming from different sources like charged lepton mass diagonalization, for example. Several such scenarios have been widely discussed in Refs. [15,16], and the latest neutrino oscillation data can be successfully predicted within the framework of many interesting flavor symmetry models.

Apart from the origin of neutrino mass and mixing, the observed matter antimatter asymmetry also remain unexplained within the SM framework. The observed baryon asymmetry in the Universe is encoded in the baryon-to-photon ratio measured by dedicated cosmology experiments like Wilkinson Mass Anisotropy Probe, Planck, etc. The latest data available from the Planck mission constrain the baryon-to-photon ratio [17] as

$$Y_B \simeq (6.065 \pm 0.090) \times 10^{-10}. \quad (1)$$

Leptogenesis is one of the most widely studied mechanisms of generating this observed baryon asymmetry in the Universe by generating an asymmetry in the leptonic sector first and later converting it into baryon asymmetry through electroweak sphaleron transitions [18]. As pointed out first by Fukugita and Yanagida [19], the out-of-equilibrium  $CP$ -violating decay of heavy Majorana neutrinos provides a natural way to create the required lepton asymmetry. The salient feature of this mechanism is the way it relates two of the most widely studied problems in particle physics: the origin of neutrino mass and the origin of matter-antimatter asymmetry. This idea has been implemented in several interesting models in the literature [20–22]. Recently, such a comparative study was done to understand the impact of mass hierarchies, Dirac and Majorana  $CP$  phases on the predictions for baryon asymmetry in Ref. [23] within the framework of left-right symmetric models.

In the present work, we propose a common mechanism that can generate the desired neutrino mass and mixing including nonzero  $\theta_{13}$  and also the matter-antimatter asymmetry. We extend the SM by three right-handed singlet neutrinos and one Higgs triplet such that both type I and type II seesaws can contribute to neutrino mass. The type I seesaw is assumed to give rise to a  $\mu - \tau$  symmetric neutrino mass matrix with  $\theta_{13} = 0$ , whereas the type II seesaw acts as a perturbation that breaks the  $\mu - \tau$  symmetry resulting in nonzero  $\theta_{13}$ . Similar works have been done recently in which the type II seesaw was considered to be the origin of  $\theta_{13}$  [24] as well as nonzero Dirac  $CP$  phase  $\delta$  [25] by assuming the type I seesaw giving rise to TBM-type mixing. Some earlier works studying neutrino masses and mixing by using the interplay of two different seesaw mechanisms can be found in Refs. [26–28]. In this work, we generalize earlier studies on TBM-type mixing to most general  $\mu - \tau$  symmetric neutrino mass matrices and check whether a minimal form

of the  $\mu - \tau$  symmetry breaking type II seesaw can give rise to the correct value of reactor mixing angle  $\theta_{13}$ . We then calculate the predictions for other neutrino parameters as well as observables like the sum of absolute neutrino masses  $\sum_i |m_i|$  and effective neutrino mass  $m_{ee} = |\sum_i U_{ei}^2 m_i|$ . We check whether the sum of absolute neutrino masses obeys the cosmological upper bound  $\sum_i |m_i| < 0.23$  eV [17] and whether the effective neutrino mass  $m_{ee}$  lies within the bounds coming from neutrinoless double beta decay experiments. We also calculate the lepton asymmetry by considering the source of leptonic Dirac  $CP$  violation in the charged lepton sector. From the requirement of generating correct neutrino parameters and baryon asymmetry, we constrain type II seesaw strength and the Dirac  $CP$  phase, and at the same time discriminate between neutrino mass hierarchies, different lightest neutrino masses, and different  $\mu - \tau$  symmetric mass matrices.

To that end, the lepton flavor violating decays like  $\mu \rightarrow e\gamma$  and  $\mu \rightarrow 3e$  with mediation of the TeV scale Higgs triplet scalar has been carefully examined. In the present work, we have considered the type II seesaw contribution to light neutrino mass  $m_\nu = f_\nu v_\Delta$ , where  $v_\Delta \simeq \mu_{\Phi\Delta} v^2 / \sqrt{2} M^2$  is the induced vacuum expectation value (VEV) of the neutral component of the Higgs triplet scalar, as a subdominant term (of the order of 0.001 eV) as compared to the dominant type I seesaw contribution. If  $f_\nu$  is assumed to be taken at its natural value  $\mathcal{O}(0.1-1.0)$ , then sub-eV scale light neutrino mass can be generated in a twofold way: (i) either by a large Higgs triplet mass  $M_\Delta$  [9] or (ii) by a small value of  $\mu_{\Phi\Delta}$ . It makes the possibility of probing the standard type II seesaw mechanism at high-energy accelerator experiments with large seesaw scale  $M_\Delta > 10^{13}$  GeV and the associated lepton flavor violating (LFV) processes heavily suppressed. Alternatively, if the type II seesaw mechanism is operative at the TeV scale, then the resulting LFV processes are prominent, and same-sign dilepton signatures are one of the prime focuses at the LHC. Within the low scale type II setup, the seesaw relation for Higgs triplet VEV is consistent with small trilinear mass term  $\mu_{\Phi\Delta}$  and the TeV scale Higgs scalar triplet mass. We wish to examine the associated LFV processes that can originate via the Higgs triplet scale, and the corresponding branching ratios for them are significant enough to be probed at ongoing search experiments if the mass of the triplet scalar is in the TeV range.

The plan of the paper is sketched in the following manner. In Sec. II, we discuss the methodology of the type I and type II seesaw mechanisms. In Sec. III, we discuss the parametrization of different  $\mu - \tau$  symmetric neutrino mass matrices. We then discuss deviations from  $\mu - \tau$  symmetry using the type II seesaw in Sec. IV. In Sec. V, we discuss  $CP$  violation and outline the mechanism of leptogenesis in the presence of the type I and type II seesaws. In Sec. VII, we discuss our numerical analysis and results and then finally conclude in Sec. VIII.

## II. SEESAW MECHANISM: TYPE I AND TYPE II

The type I seesaw [8] mechanism is the simplest possible realization of the dimension-5 Weinberg operator [29] for the origin of neutrino masses within a renormalizable framework. This mechanism is implemented in the standard model by the inclusion of three additional right-handed neutrinos ( $\nu_R^i, i = 1, 2, 3$ ) as  $SU(2)_L$  singlets with zero  $U(1)_Y$  charges. Being singlet under the gauge group, bare mass terms of the right-handed neutrinos  $M_{RR}$  are allowed in the Lagrangian. On the other hand, in the type II seesaw [9] mechanism, the standard model is extended by inclusion of an additional  $SU(2)_L$  triplet scalar field  $\Delta$  having  $U(1)_Y$  charge twice that of lepton doublets with its  $2 \times 2$  matrix representation as

$$\Delta = \begin{pmatrix} \Delta^+/\sqrt{2} & \Delta^{++} \\ \Delta^0 & -\Delta^+/\sqrt{2} \end{pmatrix}.$$

Thus, the gauge-invariant Lagrangian relevant for the type I plus type II seesaw mechanism is given as

$$\mathcal{L} = (D_\mu \Phi)^\dagger (D^\mu \Phi) + \text{Tr}(D_\mu \Delta)^\dagger (D^\mu \Delta) - \mathcal{L}_Y^{\text{lept}} - V(\Phi, \Delta), \quad (2)$$

with the leptonic interaction terms,

$$\mathcal{L}_Y = y_{ij} \ell_i \tilde{\Phi} \nu_{Rj} + f_{ij} \ell_i^T C (i\tau_2) \Delta \ell_j + \frac{1}{2} \nu_R^T C^{-1} M_{RR} \nu_R + \text{h.c.} \quad (3)$$

Here,  $\ell_L \equiv (\nu, e)_L^T$ ,  $\Phi \equiv (\phi^0, \phi^-)^T$ , and  $C$  is the charge conjugation operator. The scalar potential of the model using the SM Higgs doublet  $\Phi$  and Higgs triplet scalar  $\Delta_L$  is

$$\begin{aligned} \mathcal{V}(\Phi, \Delta) &= \mu_\Phi^2 \Phi^\dagger \Phi + \lambda_1 (\Phi^\dagger \Phi)^2 + \mu_\Delta^2 \text{Tr}(\Delta^\dagger \Delta) \\ &+ \lambda_2 [\text{Tr}(\Delta^\dagger \Delta)]^2 + \lambda_3 \text{Det}(\Delta^\dagger \Delta) \\ &+ \lambda_4 (\Phi^\dagger \Phi) \text{Tr}(\Delta^\dagger \Delta) + \lambda_5 (\Phi^\dagger \tau_i \Phi) \text{Tr}(\Delta^\dagger \tau_i \Delta) \\ &+ \frac{1}{\sqrt{2}} \mu_{\Phi\Delta} (\Phi^T i\tau_2 \Delta \Phi) + \text{h.c.} \end{aligned} \quad (4)$$

With the vacuum expectation value of the SM Higgs  $\langle \Phi^0 \rangle = v/\sqrt{2}$ , the trilinear mass term  $\mu_{\Phi\Delta}$  generates an induced VEV for the Higgs triplet as  $\langle \Delta^0 \rangle = v_\Delta/\sqrt{2}$  where  $v_\Delta \simeq \mu_{\Phi\Delta} v^2/\sqrt{2}M_\Delta^2$ , and the resulting  $6 \times 6$  neutrino mass matrix after electroweak symmetry breaking reads as

$$\mathcal{M}_\nu = \begin{pmatrix} m_{LL} & m_{LR} \\ m_{LR}^T & M_{RR} \end{pmatrix}, \quad (5)$$

where  $m_{LR} = y_\nu v$  is the Dirac neutrino mass,  $m_{LL} = f_\nu v_\Delta$  is the Majorana mass for light active neutrinos, and  $m_{RR}$  is

the bare mass term for heavy sterile Majorana neutrinos. Within the mass hierarchy  $M_{RR} \gg m_{LR} \gg m_{LL}$ , the seesaw formula for the light neutrino mass is given by

$$m_\nu \equiv m_{LL} = m_{LL}^I + m_{LL}^{II}, \quad (6)$$

where the formula for the type I seesaw contribution is presented as

$$m_{LL}^I = -m_{LR} M_{RR}^{-1} m_{LR}^T, \quad (7)$$

where  $m_{LR}$  is the Dirac mass term of the neutrinos that is typically of the electroweak scale. Demanding the light neutrinos to be of the eV scale, one needs  $M_{RR}$  to be as high as  $10^{14}$  GeV without any fine-tuning of Dirac Yukawa couplings, whereas the type II seesaw contribution to the light neutrino mass is given by

$$m_{LL}^{II} = f_\nu v_\Delta, \quad (8)$$

where the analytic formula for the induced VEV for a neutral component of the Higgs scalar triplet, derived from the minimization of the scalar potential, is

$$v_\Delta \equiv \langle \Delta^0 \rangle = \frac{\mu_{\Phi\Delta} v^2}{M_\Delta^2}. \quad (9)$$

In the low scale type II seesaw mechanism operative at the TeV scale, barring the naturalness issue, one can consider a very small value of the trilinear mass parameter to be

$$\mu_{\Phi\Delta} \simeq 10^{-8} \text{ GeV},$$

where the Higgs scalar triplet mass lies within the TeV range, which gives the interesting phenomenological possibility of being produced in pairs at LHC. The sub-eV scale light neutrino mass with type II seesaw mechanism constrains the corresponding Majorana Yukawa coupling as

$$f_\nu^2 < 1.4 \times 10^{-5} \left( \frac{M_\Delta}{1 \text{ TeV}} \right).$$

Within the reasonable value of  $f_\nu \simeq 10^{-2}$ , the triplet Higgs scalar VEV is  $v_\Delta \simeq 10^{-7}$  GeV, which is in agreement with the oscillation data. It is worth noting here that the tiny trilinear mass parameter  $\mu_{\Phi\Delta}$  controls the neutrino overall mass scale but does not play any role in the couplings with the fermions, thereby making the lepton flavor violation studies more viable.

## III. $\mu - \tau$ SYMMETRIC NEUTRINO MASS MATRIX

The  $\mu - \tau$  symmetric neutrino mass matrix is one of the most widely studied neutrino mixing scenario in the

literature. In this work, we consider four different types of  $\mu - \tau$  symmetric neutrino mass matrices: BM, TBM, HM, and GRM. These scenarios predict  $\theta_{13} = 0, \theta_{23} = \frac{\pi}{4}$ , whereas the value of  $\theta_{12}$  depends upon the particular model. Since  $\theta_{13} = 0$  has been ruled out by latest neutrino oscillation experiments, the  $\mu - \tau$  symmetry has to be broken appropriately in order to account for the correct neutrino oscillation data. We assume these four different  $\mu - \tau$  symmetric neutrino mass matrices to originate from the type I seesaw mechanism, whereas the type II seesaw term acts as a perturbation that breaks  $\mu - \tau$  symmetry in order to produce the correct neutrino oscillation parameters.

The  $\mu - \tau$  symmetric BM-type neutrino mass matrix originating from the type I seesaw can be parametrized as

$$m_{LL} = \begin{pmatrix} A+B & F & F \\ F & A & B \\ F & B & A \end{pmatrix}. \quad (10)$$

This has eigenvalues  $m_1 = A+B+\sqrt{2}F, m_2 = A+B-\sqrt{2}F$ , and  $m_3 = A-B$ . It predicts the mixing angles as  $\theta_{23} = \theta_{12} = 45^\circ$  and  $\theta_{13} = 0$ . It clearly shows that only the first mixing angle  $\theta_{23}$  is still allowed from oscillation data, whereas  $\theta_{12} = 45^\circ$  and  $\theta_{13} = 0$  have been ruled out experimentally.

The  $\mu - \tau$  symmetric TBM-type neutrino mass matrix originating from the type I seesaw can be parametrized as

$$m_{LL} = \begin{pmatrix} A & B & B \\ B & A+F & B-F \\ B & B-F & A+F \end{pmatrix}, \quad (11)$$

which is clearly  $\mu - \tau$  symmetric with eigenvalues  $m_1 = A-B, m_2 = A+2B$ , and  $m_3 = A-B+2F$ . It predicts the mixing angles as  $\theta_{12} \simeq 35.3^\circ, \theta_{23} = 45^\circ$ , and  $\theta_{13} = 0$ . Although the predictions for first two mixing angles are still allowed from oscillation data,  $\theta_{13} = 0$  has been ruled out experimentally at more than  $9\sigma$  confidence level.

In the same way, the  $\mu - \tau$  symmetric HM-type neutrino mass matrix can be written as

$$m_{LL} = \begin{pmatrix} A & B & B \\ B & \frac{1}{2}(A+2\sqrt{\frac{2}{3}}B+F) & \frac{1}{2}(A+2\sqrt{\frac{2}{3}}B-F) \\ B & \frac{1}{2}(A+2\sqrt{\frac{2}{3}}B-F) & \frac{1}{2}(A+2\sqrt{\frac{2}{3}}B+F) \end{pmatrix}. \quad (12)$$

This has eigenvalues  $m_1 = \frac{1}{3}(3A - \sqrt{6}B), m_2 = A + \sqrt{6}B$ , and  $m_3 = F$ . This predicts the mixing angles to be  $\theta_{23} = 45^\circ, \theta_{12} = 30^\circ$ , and  $\theta_{13} = 0$ . Oscillation data still allow  $\theta_{23} = 45^\circ$  and  $\theta_{12} = 30^\circ$ , whereas  $\theta_{13} = 0$  is ruled

out. For the GRM pattern, the  $\mu - \tau$  symmetric neutrino mass matrix can be written as

$$m_{LL} = \begin{pmatrix} A & B & B \\ B & F & A + \sqrt{2}B - F \\ B & A + \sqrt{2}B - F & F \end{pmatrix}, \quad (13)$$

giving the eigenvalues equal to  $m_1 = \frac{1}{2}(2A + \sqrt{2}B - \sqrt{10}B), m_2 = \frac{1}{2}(2A + \sqrt{2}B + \sqrt{10}B)$ , and  $m_3 = -A - \sqrt{2}B + 2F$ . This gives rise to neutrino mixing angles as  $\theta_{23} = 45^\circ, \theta_{12} = 31.71^\circ$ , and  $\theta_{13} = 0$ . Apart from  $\theta_{13}$ , the other two mixing angles are still within the  $3\sigma$  range of neutrino mixing angles.

#### IV. DEVIATIONS FROM $\mu - \tau$ SYMMETRY

For simplicity, we assume the type II seesaw mass matrix to be of minimal form while ensuring, at the same time, that it breaks the  $\mu - \tau$  symmetry in order to generate nonzero  $\theta_{13}$ . The form of the neutrino mass matrix arising from type II seesaw only is taken as

$$m_{LL}^I = \begin{pmatrix} 0 & -w & w \\ -w & w & 0 \\ w & 0 & -w \end{pmatrix}. \quad (14)$$

The structure of this mass matrix, although it looks *ad hoc*, can, however, be explained within generic flavor symmetry models like  $A_4$ . Within the framework of the seesaw mechanism, neutrino mass and mixing have been extensively studied by many authors using discrete flavor symmetries [30] available in the literature. Among the different discrete flavor symmetry groups, the group of even permutations on four elements  $A_4$  can naturally explain the  $\mu - \tau$  symmetric mass matrix obtained from the type I seesaw mechanism. Without going into the details of generating a  $\mu - \tau$  symmetric mass matrix within  $A_4$  models, an exercise performed already by several authors, here we briefly outline one possible way of generating the type II seesaw mass matrix (14) within an  $A_4$  model. This group has 12 elements having 4 irreducible representations, with dimensions  $n_i$ , such that  $\sum_i n_i^2 = 12$ . The characters of the four representations are shown in Table VII. The complex number  $\omega$  is the cube root of unity. The group  $A_4$  has four irreducible representations, namely,  $\mathbf{1}, \mathbf{1}', \mathbf{1}''$ , and  $\mathbf{3}$ . In generic  $A_4$  models, the  $SU(2)_L$  lepton doublets  $l = (l_e, l_\mu, l_\tau)$  are assumed to transform as triplet  $\mathbf{3}$  under  $A_4$ , whereas the  $SU(2)_L$  singlet charged leptons  $e^c, \mu^c, \tau^c$  transform as  $\mathbf{1}, \mathbf{1}', \mathbf{1}''$ , respectively. In type I seesaw scenarios, the  $SU(2)_L$  singlet right-handed neutrinos  $\nu^c$  transform as a triplet under  $A_4$ . Since we are trying to explain the structure of the type II term only, we confine our discussion to the lepton doublets only. We introduce three scalars  $\zeta_1, \zeta_2, \zeta_3$  transforming as  $\mathbf{1}, \mathbf{1}', \mathbf{1}''$  under  $A_4$ . The



$SU(2)_L$  triplet Higgs field  $\Delta_L$  is assumed to be a singlet under  $A_4$ . Thus, the type II seesaw term can be written as

$$\mathcal{L}^H = f ll(\zeta_1 + \zeta_2 + \zeta_3)\Delta_L/\Lambda,$$

where  $\Lambda$  is the cutoff scale and  $f$  is a dimensionless coupling constant.

The decomposition of the  $ll\zeta_{1,2,3}$  terms into the  $A_4$  singlet gives

$$\begin{aligned} ll\zeta_1 &= (l_e l_e + l_\mu l_\tau + l_\tau l_\mu)\zeta_1 \\ ll\zeta_2 &= (l_\mu l_\mu + l_e l_\tau + l_\tau l_e)\zeta_2 \\ ll\zeta_3 &= (l_\tau l_\tau + l_e l_\mu + l_\mu l_e)\zeta_3. \end{aligned}$$

Assuming the vacuum alignments of the scalars as  $\langle\zeta_1\rangle = 0$ ,  $\langle\zeta_2\rangle = \Lambda$ ,  $\langle\zeta_3\rangle = -\Lambda$ , we obtain the type II seesaw contribution to neutrino mass as

$$m_{LL}^H = \begin{pmatrix} 0 & -f\langle\delta_L^0\rangle & f\langle\delta_L^0\rangle \\ -f\langle\delta_L^0\rangle & f\langle\delta_L^0\rangle & 0 \\ f\langle\delta_L^0\rangle & 0 & -f\langle\delta_L^0\rangle \end{pmatrix}, \quad (15)$$

which has the same form as (14) if we denote  $f\langle\delta_L^0\rangle = f v_L$  as  $w$ . We adopt this minimal structure of the type II seesaw mass matrix for our numerical analysis.

## V. CP VIOLATION AND LEPTOGENESIS

Leptogenesis is one of the most widely studied mechanisms to generate the observed baryon asymmetry of the Universe by creating an asymmetry in the leptonic sector first, which subsequently gets converted into baryon

asymmetry through  $B + L$ -violating sphaleron processes during electroweak phase transition. Since quark sector  $CP$  violation is not sufficient for producing observed baryon asymmetry, a framework explaining nonzero  $\theta_{13}$  and the leptonic  $CP$  phase could not only give a better picture of leptonic flavor structure but also the origin of matter-antimatter asymmetry.

In a model with both type I and type II seesaw mechanisms at work, there are two possible sources of lepton asymmetry: either the  $CP$ -violating decay of the lightest right-handed neutrino or that of the scalar triplet. Recently, such a work was performed in Ref. [23], where the contributions of the type I and type II seesaws to baryon asymmetry were calculated without assuming any specific symmetries in the type I or type II seesaw matrices. In another work [25], the type II seesaw was considered to be the origin of the nonzero  $\theta_{13}$  and nontrivial Dirac  $CP$  phase simultaneously, and baryon asymmetry was calculated taking the contribution only from the type II seesaw term. In the present work, both type I and type II seesaw mass matrices are real, and hence the diagonalizing matrix  $U_\nu$  of neutrino mass matrix is also real, giving rise to trivial values of the Dirac  $CP$  phase. Thus, the only remaining source of  $CP$  violation in the leptonic sector is the charged lepton sector. We note that the Pontecorvo–Maki–Nakagawa–Sakata (PMNS) leptonic mixing matrix is related to the diagonalizing matrices of neutrino and charged lepton mass matrices  $U_\nu$ ,  $U_l$ , respectively, as

$$U_{\text{PMNS}} = U_l^\dagger U_\nu. \quad (16)$$

The PMNS mixing matrix can be parametrized as

$$U_{\text{PMNS}} = \begin{pmatrix} c_{12}c_{13} & s_{12}c_{13} & s_{13}e^{-i\delta} \\ -s_{12}c_{23} - c_{12}s_{23}s_{13}e^{i\delta} & c_{12}c_{23} - s_{12}s_{23}s_{13}e^{i\delta} & s_{23}c_{13} \\ s_{12}s_{23} - c_{12}c_{23}s_{13}e^{i\delta} & -c_{12}s_{23} - s_{12}c_{23}s_{13}e^{i\delta} & c_{23}c_{13} \end{pmatrix}, \quad (17)$$

where  $c_{ij} = \cos\theta_{ij}$ ,  $s_{ij} = \sin\theta_{ij}$ , and  $\delta$  is the Dirac  $CP$  phase. Our goal is to generate correct values of neutrino mixing angles including nonzero  $\theta_{13}$  with the combination of type I and type II seesaws. Since, the neutrino mass matrix is real without any phase, its diagonalizing matrix  $U_\nu$  is also real and takes the form of  $U_{\text{PMNS}}$  after setting  $\delta$  to zero. Thus, the charged lepton mass diagonalizing matrix  $U_l$ , the only source of nonzero  $CP$  phase  $\delta$ , can be written as

$$U_l = \begin{pmatrix} c_{13}^2 + e^{i\delta}s_{13}^2 & (1 - e^{-i\delta})c_{13}s_{13}s_{23} & (1 - e^{-i\delta})c_{13}s_{13}c_{23} \\ (-1 + e^{i\delta})c_{13}s_{13}s_{23} & c_{13}^2 + s_{13}^2(c_{23}^2 + e^{-i\delta}s_{23}^2) & (-1 + e^{-i\delta})c_{23}s_{13}^2s_{23} \\ (-1 + e^{i\delta})c_{13}s_{13}c_{23} & (-1 + e^{-i\delta})c_{23}s_{13}^2s_{23} & c_{13}^2 + s_{13}^2(s_{23}^2 + e^{-i\delta}c_{23}^2) \end{pmatrix}. \quad (18)$$

We derive this form of  $U_l$  such that  $U_l^\dagger U_\nu$  gives the desired form of the PMNS mixing matrix (17). If we assume that this matrix  $U_l$  also diagonalizes the Dirac neutrino mass matrix  $m_{LR}$ , the  $CP$  phase originating in the charged lepton sector can affect the lepton asymmetry as we discuss below.

In our work, we are considering  $CP$ -violating out-of-equilibrium decay of heavy right-handed neutrinos into a Higgs and lepton within the framework of the dominant type I and subdominant type II seesaw mechanisms. In principle, the decay of the Higgs triplet having masses a few hundred GeV can contribute to the  $CP$  asymmetry in the lepton sector having prominent gauge interaction along with the as usual  $CP$  asymmetry due to heavy ( $> 10^9$  GeV) right-handed neutrino decays without having any gauge interaction. The washout factors in the case of  $CP$  asymmetry due to triplet decay are large, and thus the net  $CP$  asymmetry is negligible. For simplicity, we consider only the right-handed neutrino decay as a source of lepton asymmetry and neglect the contribution coming from triplet decay. The lepton asymmetry from the decay of the right-handed neutrino into leptons and a Higgs scalar is given by

$$\epsilon_{N_k} = \sum_i \frac{\Gamma(N_k \rightarrow L_i + H^*) - \Gamma(N_k \rightarrow \bar{L}_i + H)}{\Gamma(N_k \rightarrow L_i + H^*) + \Gamma(N_k \rightarrow \bar{L}_i + H)}. \quad (19)$$

In a hierarchical pattern for right-handed neutrinos  $M_{2,3} \gg M_1$ , it is sufficient to consider the lepton asymmetry produced by the decay of lightest right-handed neutrino  $N_1$  decay. In a type I seesaw framework where the particle content is just the standard model with three additional right-handed neutrinos, the lepton asymmetry is generated through the decay processes shown in Fig. 1. In the presence of the type II seesaw,  $N_1$  can also decay through a virtual triplet as can be seen in Fig. 2. Following the notations of Ref. [21], the lepton asymmetry arising from the decay of  $N_1$  in the presence of the type I seesaw only can be written as

$$\begin{aligned} \epsilon_1^\alpha &= \frac{1}{8\pi v^2} \frac{1}{(m_{LR}^\dagger m_{LR})_{11}} \\ &\times \sum_{j=2,3} \text{Im}[(m_{LR}^*)_{\alpha 1} (m_{LR}^\dagger m_{LR})_{1j} (m_{LR})_{\alpha j}] g(x_j) \\ &+ \frac{1}{8\pi v^2} \frac{1}{(m_{LR}^\dagger m_{LR})_{11}} \\ &\times \sum_{j=2,3} \text{Im}[(m_{LR}^*)_{\alpha 1} (m_{LR}^\dagger m_{LR})_{j1} (m_{LR})_{\alpha j}] \frac{1}{1-x_j}, \quad (20) \end{aligned}$$

where  $v = 174$  GeV is the VEV of the Higgs bidoublets responsible for breaking the electroweak symmetry,

$$g(x) = \sqrt{x} \left( 1 + \frac{1}{1-x} - (1+x) \ln \frac{1+x}{x} \right),$$

and  $x_j = M_j^2/M_1^2$ . The second term in the expression for  $\epsilon_1^\alpha$  above vanishes when summed over all the flavors  $\alpha = e, \mu, \tau$ . The sum over flavors is given by

$$\epsilon_1 = \frac{1}{8\pi v^2} \frac{1}{(m_{LR}^\dagger m_{LR})_{11}} \sum_{j=2,3} \text{Im}[(m_{LR}^\dagger m_{LR})_{1j}^2] g(x_j). \quad (21)$$

After determining the lepton asymmetry  $\epsilon_1$ , the corresponding baryon asymmetry can be obtained by

$$Y_B = c\kappa \frac{\epsilon}{g_*} \quad (22)$$

through electroweak sphaleron processes [18]. Here, the factor  $c$  is a measure of the fraction of lepton asymmetry being converted into baryon asymmetry and is approximately equal to  $-0.55$ .  $\kappa$  is the dilution factor due to the washout process that erases the produced asymmetry and can be parametrized as [31]

$$\begin{aligned} -\kappa &\simeq \sqrt{0.1K} \exp[-4/(3(0.1K)^{0.25})], \quad \text{for } K \geq 10^6 \\ &\simeq \frac{0.3}{K(\ln K)^{0.6}}, \quad \text{for } 10 \leq K \leq 10^6 \\ &\simeq \frac{1}{2\sqrt{K^2+9}}, \quad \text{for } 0 \leq K \leq 10, \quad (23) \end{aligned}$$

where  $K$  is given as

$$K = \frac{\Gamma_1}{H(T=M_1)} = \frac{(m_{LR}^\dagger m_{LR})_{11} M_1}{8\pi v^2} \frac{M_{Pl}}{1.66\sqrt{g_*} M_1^2}.$$

Here,  $\Gamma_1$  is the decay width of  $N_1$ , and  $H(T=M_1)$  is the Hubble constant at temperature  $T=M_1$ . The factor  $g_*$  is the effective number of relativistic degrees of freedom at  $T=M_1$  and is approximately 110.

We note that the lepton asymmetry shown in Eq. (21) is obtained by summing over all the flavors  $\alpha = e, \mu, \tau$ . A nonvanishing lepton asymmetry is generated only when the right-handed neutrino decay is out of equilibrium. Otherwise, both the forward and the backward processes will happen at the same rate, resulting in a vanishing asymmetry. Departure from equilibrium can be estimated by comparing the interaction rate with the expansion rate of the Universe. At very high temperatures ( $T \geq 10^{12}$  GeV), all charged lepton flavors are out of equilibrium, and hence all of them behave similarly resulting in the one-flavor regime. However, at temperatures  $T < 10^{12}$  GeV ( $T < 10^9$  GeV), interactions involving tau (muon) Yukawa couplings enter equilibrium, and flavor effects become important [32]. Taking these flavor effects into account, the final baryon asymmetry is given by

$$Y_B^{2\text{flavor}} = \frac{-12}{37g^*} \left[ \epsilon_2 \eta \left( \frac{417}{589} \tilde{m}_2 \right) + \epsilon_1^\tau \eta \left( \frac{390}{589} \tilde{m}_\tau \right) \right]$$

$$Y_B^{3\text{flavor}} = \frac{-12}{37g^*} \left[ \epsilon_1^\epsilon \eta \left( \frac{151}{179} \tilde{m}_e \right) + \epsilon_1^\mu \eta \left( \frac{344}{537} \tilde{m}_\mu \right) + \epsilon_1^\tau \eta \left( \frac{344}{537} \tilde{m}_\tau \right) \right],$$

where  $\epsilon_2 = \epsilon_1^\epsilon + \epsilon_1^\mu$ ,  $\tilde{m}_2 = \tilde{m}_e + \tilde{m}_\mu$ ,  $\tilde{m}_\alpha = \frac{(m_{LR}^*)_{1\alpha}(m_{LR})_{\alpha 1}}{M_1}$ . The function  $\eta$  is given by

$$\eta(\tilde{m}_\alpha) = \left[ \left( \frac{\tilde{m}_\alpha}{8.25 \times 10^{-3} \text{ eV}} \right)^{-1} + \left( \frac{0.2 \times 10^{-3} \text{ eV}}{\tilde{m}_\alpha} \right)^{-1.16} \right]^{-1}.$$

In the presence of an additional scalar triplet, the right-handed neutrino can also decay through a virtual triplet as shown in Fig. 2. The contribution of this diagram to lepton asymmetry can be estimated as [33]

$$\epsilon_{\Delta 1}^\alpha = -\frac{M_1}{8\pi v^2} \frac{\sum_{j=2,3} \text{Im}[(m_{LR})_{1j}(m_{LR})_{1\alpha}(M_\nu^{II*})_{j\alpha}]}{\sum_{j=2,3} |(m_{LR})_{1j}|^2}. \quad (24)$$

For the calculation of baryon asymmetry, we go to the basis in which the right-handed Majorana neutrino mass matrix is diagonal:

$$U_R^* M_{RR} U_R^\dagger = \text{diag}(M_1, M_2, M_3). \quad (25)$$

In this diagonal  $M_{RR}$  basis, the Dirac neutrino mass matrix also changes to

$$m_{LR} = m_{LR}^0 U_R, \quad (26)$$

where  $m_{LR}^0$  is the Dirac neutrino mass matrix given by

$$m_{LR}^0 = U_I m_{LR}^d U_I^\dagger. \quad (27)$$

Here,  $m_{LR}^d$  is the diagonal form of the Dirac neutrino mass matrix in our calculation given by

$$m_{LR}^d = \begin{pmatrix} \lambda^m & 0 & 0 \\ 0 & \lambda^n & 0 \\ 0 & 0 & 1 \end{pmatrix} m_f, \quad (28)$$

where  $\lambda = 0.22$  is the standard Wolfenstein parameter and  $(m, n)$  are positive integers. As mentioned earlier,  $U_I$  is the matrix that is assumed to diagonalize both the charged lepton and Dirac neutrino mass matrices.

## VI. LEPTON FLAVOR VIOLATION

It is known that neutrino flavor is violated in the neutrino sector from the experimental observed oscillation phenomena. In the previous sections, we have presented the model

for explaining the nonzero values of reactor mixing angle  $\theta_{13}$ , as revealed from a recent oscillation experiment, by perturbation method. The idea is to take the type I seesaw contribution as the leading term in the neutrino mass matrix with the various choices for mixing matrices such as bimaximal, tribimaximal, hexagonal, and golden ratio types with uniquely predicting  $\theta_{13} = 0$ . In the second step, the nonzero value for reactor mixing angle can be found by adding a small perturbation matrix (type II seesaw term in the present work) parametrized by  $\omega$  to the leading-order mass matrix (type I seesaw term). It is numerically examined that the overall scale of the perturbation  $\omega$  is derived to be the order of 0.001 eV.

The analytic expression for the Higgs triplet VEV generated from the trilinear mass term  $\mu_{\Phi\Delta}$  in the scalar Lagrangian given in Eq. (4) is given as

$$v_\Delta = \mu_{\Phi\Delta} v^2 / \sqrt{2} M^2, \quad (29)$$

with  $v^2 = v^2 + v_\Delta^2 \simeq (174 \text{ GeV})^2$ . The resulting mass formula for neutrino mass is  $m_\nu = f_\nu v_\Delta$ . The numerical value of the perturbation term  $\omega = f_\nu v_\Delta$  crucially depends upon the Majorana coupling  $f_\nu$ , trilinear mass parameter  $\mu_{\Phi\Delta}$ , and  $M$ , which is fixed around the TeV scale. Thus, the required value of  $\omega = 0.001 \text{ eV}$  can be easily obtained by choosing these parameters appropriately. We intend to examine possible lepton flavor violation within the present framework with the TeV scale scalar triplet.

Within the present framework having the type I + type II seesaw mechanism having the TeV scale Higgs triplet and heavy right-handed Majorana neutrinos, there are various Feynman diagrams contributing to the LFV processes like  $\mu \rightarrow e\gamma$ ,  $\mu \rightarrow eee$ , and  $\mu \rightarrow e$  conversions inside a nucleus. They are arising from exchange of (i) light neutrino exchange, (ii) heavy neutrinos through light-heavy neutrino mixing proportional to  $M_D/M_R$ , and (iii) charged Higgs scalars. The light neutrino contribution is heavily suppressed ( $\text{Br}(\mu \rightarrow e\gamma) \simeq 10^{-50}$ ) and heavy neutrino contribution is very much suppressed as well due to large mass for a right-handed Majorana neutrino,  $M_R > 10^9 \text{ GeV}$ . Thus, the Higgs triplet scalar with TeV mass range can contribute to various LFV processes as shown in Fig. 3 for  $\mu \rightarrow e\gamma$  and Fig. 4 for  $\mu \rightarrow eee$ ,

$$\text{Br}_{\mu \rightarrow e+\gamma}^{\text{triplet}} \simeq 0.01 \times \frac{M_{W_L}^4}{g_L^4} \left| \frac{(f^* f)_{21}}{M_{\Delta_L^{++}}^2} \right|^2$$

$$\simeq 0.01 \times \frac{v^4}{v_\Delta^4} \left| \frac{(m_\nu^{II} m_\nu^{II\dagger})_{12}}{M_{\Delta_L^{++}}^2} \right|^2, \quad (30)$$

where we have used  $M_{W_L} \simeq 1/2g_L v$  and  $m_\nu^{II} \equiv \omega \simeq \mathcal{O}(0.001) \text{ eV}$ . Using  $v_\Delta \simeq 10^{-5} - 10^{-9} \text{ GeV}$ ,  $v \simeq 174 \text{ GeV}$ , and a doubly charged Higgs scalar mass around 300 GeV, the model prediction for  $\text{Br}_{\mu \rightarrow e+\gamma}^{\text{triplet}}$  is found to be

$\text{Br}(\mu \rightarrow e + \gamma)|_{\text{theory}} < 4.2 \times 10^{-15}$ . The current experimental constraint on  $\mu \rightarrow e\gamma$  is

$$\text{Br}(\mu \rightarrow e + \gamma)|_{\text{expt}} < 2.4 \times 10^{-12}$$

at 90% C.L. [34] Although the predicted value of the branching ratio for LFV decays  $\mu \rightarrow e\gamma$  is beyond the reach of current experimental sensitivity (for more details, see Refs. [35,36]), it is hoped that it can be probed at a future experiment [37] that is planned to reach  $\text{Br}(\mu \rightarrow e + \gamma)|_{\text{future}} \simeq \times 10^{-16}$ .

Another important LFV decay is  $\mu \rightarrow 3e$ , shown in Fig. 4, for which the branching ratio is found to be

$$\text{Br}_{\mu \rightarrow 3e}^{\text{triplet}} \simeq \frac{1}{2} \frac{M_{W_L}^4}{g_L^4} \left| \frac{(ff^\dagger)_{12}}{M_{\Delta_L^{++}}^2} \right|^2 \simeq \frac{1}{2} \frac{v^4}{v_\Delta^4} \left| \frac{(m_\nu^I m_\nu^{I\dagger})_{12}}{M_{\Delta_L^{++}}^2} \right|^2. \quad (31)$$

For numerical evaluation, consider  $v_\Delta \simeq \text{eV}$ ,  $f \simeq 10^{-3.5}$ , and  $M_{\Delta_L^{++}} \simeq (300\text{--}1000) \text{ GeV}$  results  $\text{Br}(\mu \rightarrow 3e) \simeq 10^{-12}\text{--}10^{-16}$ , which is accessible to the ongoing or future planned search experiments. The present experimental upper bound for the  $\mu \rightarrow 3e$  process is  $\text{Br}(\mu \rightarrow 3e) < 1.0 \times 10^{-12}$  [38], while it is planned to reach  $\text{Br}(\mu \rightarrow 3e) < 10^{-16}$  [39].

## VII. NUMERICAL ANALYSIS

To begin with, we write down the light neutrino mass matrix  $m_{LL}$  in terms of (complex) mass eigenvalues  $m_1, m_2, m_3$ , and PMNS mixing matrix  $U_{\text{PMNS}} \equiv U$ , working in a basis in which the charged lepton mass matrix is already diagonal, as

$$m_\nu = U^* \text{diag}(m_1, m_2, m_3) U^\dagger. \quad (32)$$

The mixing matrix  $U$  is parametrized in terms of three neutrino mixing angles  $\theta_{23}, \theta_{12}$ , and  $\theta_{13}$  and a Dirac phase  $\delta$ . The two Majorana phases are absorbed in mass eigenvalues  $m_i$  instead in the mixing matrix  $U$ . Here, the two Majorana phases are simply taken to be zero for subsequent numerical analysis.

At the first step of numerical analysis, we have considered particularly four choices of  $U$  and  $m_\nu$  so that  $\theta_{13} = 0$  and  $\theta_{23}$  is maximal with the general form of the mixing matrix at leading order as

$$U = \begin{pmatrix} c_{12} & s_{12} & 0 \\ -s_{12}/\sqrt{2} & c_{12}/\sqrt{2} & -1/\sqrt{2} \\ -s_{12}/\sqrt{2} & c_{12}/\sqrt{2} & 1/\sqrt{2} \end{pmatrix}. \quad (33)$$

We start writing the relevant matrix form for light neutrino mass satisfying  $\mu - \tau$  symmetry and corresponding mixing matrix having different values of  $\theta_{12}$  but consistent with our earlier assumptions, i.e.,  $\theta_{13} = 0$  and maximal  $\theta_{23}$ , as

$$m_\nu^{(0)}|_{\text{BM}} = \begin{pmatrix} A+B & F & F \\ F & A & B \\ F & B & A \end{pmatrix},$$

$$U_{\text{BM}} = \begin{pmatrix} 1/\sqrt{2} & 1/\sqrt{2} & 0 \\ -1/2 & 1/2 & -1/\sqrt{2} \\ -1/2 & 1/2 & 1/\sqrt{2} \end{pmatrix}, \quad (34)$$

with  $m_1 = A + B + \sqrt{2}F$ ,  $m_2 = A + B - \sqrt{2}F$ ,  $m_3 = A - B$ ,

$$m_\nu^{(0)}|_{\text{TBM}} = \begin{pmatrix} A & B & B \\ B & A+F & B-F \\ B & B-F & A+F \end{pmatrix},$$

$$U_{\text{TBM}} = \begin{pmatrix} 2/\sqrt{6} & 1/\sqrt{3} & 0 \\ -1/\sqrt{6} & 1/\sqrt{3} & -1/\sqrt{2} \\ -1/\sqrt{6} & 1/\sqrt{3} & 1/\sqrt{2} \end{pmatrix}, \quad (35)$$

with  $m_1 = A - B$ ,  $m_2 = A + 2B$ , and  $m_3 = A - B + 2F$ . It is clear from the BM and TBM types of mixing matrices that

$$\tan^2 \theta_{23} = |U_{\mu 3}|^2 / |U_{\tau 3}|^2 = 1.$$

Similarly, there are two other types of the mass matrix and mixing matrix that can reproduce  $\theta_{13} = 0$  and maximal  $\theta_{23}$ , and they are (i) hexagonal-type predicting  $\theta_{12} = \pi/6$  and (ii) golden ratio type, for which  $\theta_{12} \tan^{-1}(1/\varphi)$  with  $\varphi = (1 + \sqrt{5})/2$ ,

TABLE I. Experimental value of reactor mixing angle from recent neutrino oscillation experiments.

Experimental data	$\sin^2 2\theta_{13}$	$\sin^2 \theta_{13}$
T2K [2]	$0.11^{+0.11}_{-0.05} (0.14^{+0.12}_{-0.06})$	$0.028^{+0.019}_{-0.024} (0.036^{+0.022}_{-0.030})$
Double ChooZ [3]	$0.086 \pm 0.041 \pm 0.030$	$0.022^{+0.019}_{-0.018}$
Daya-Bay [4]	$0.092 \pm 0.016 \pm 0.005$	$0.024 \pm 0.005$
RENO [5]	$0.113 \pm 0.013 \pm 0.019$	$0.029 \pm 0.006$



$$m_\nu^{(0)}|_{\text{HM}} = \begin{pmatrix} A & B & B \\ B & \frac{1}{2}(A + 2\sqrt{\frac{2}{3}}B + F) & \frac{1}{2}(A + 2\sqrt{\frac{2}{3}}B - F) \\ B & \frac{1}{2}(A + 2\sqrt{\frac{2}{3}}B - F) & \frac{1}{2}(A + 2\sqrt{\frac{2}{3}}B + F) \end{pmatrix}, \quad U_{\text{HM}} = \begin{pmatrix} \frac{\sqrt{3}}{2} & \frac{1}{2} & 0 \\ -\frac{\sqrt{2}}{4} & \frac{\sqrt{6}}{4} & -\frac{1}{\sqrt{2}} \\ -\frac{\sqrt{2}}{4} & -\frac{\sqrt{6}}{4} & \frac{1}{\sqrt{2}} \end{pmatrix},$$

with  $m_1 = \frac{1}{3}(3A - \sqrt{6}B)$ ,  $m_2 = A + \sqrt{6}B$ , and  $m_3 = F$ ,

$$m_\nu^{(0)}|_{\text{GRM}} = \begin{pmatrix} A & B & B \\ B & F & A + \sqrt{2}B - F \\ B & A + \sqrt{2}B - F & F \end{pmatrix}, \quad U_{\text{GRM}} = \begin{pmatrix} \frac{\sqrt{2}}{\sqrt{5-\sqrt{5}}} & \frac{\sqrt{2}}{\sqrt{5+\sqrt{5}}} & 0 \\ -\frac{\sqrt{2}}{\sqrt{5+\sqrt{5}}} & \frac{\sqrt{2}}{\sqrt{5-\sqrt{5}}} & -1/\sqrt{2} \\ -\frac{\sqrt{2}}{\sqrt{5+\sqrt{5}}} & \frac{\sqrt{2}}{\sqrt{5-\sqrt{5}}} & 1/\sqrt{2} \end{pmatrix},$$

TABLE II. The global fit values for the mass squared differences and mixing angles as reported by Ref. [6] presented by the second column and by Ref. [7] presented by the third column.

Oscillation parameters	Within $3\sigma$ range (Schwetz <i>et al.</i> [6])	Within $3\sigma$ range (Fogli <i>et al.</i> [7])
$\Delta m_{21}^2 [10^{-5} \text{ eV}^2]$	7.00–8.09	6.99–8.18
$ \Delta m_{31}^2(\text{NH})  [10^{-3} \text{ eV}^2]$	2.27–2.69	2.19–2.62
$ \Delta m_{23}^2(\text{IH})  [10^{-3} \text{ eV}^2]$	2.24–2.65	2.17–2.61
$\sin^2 \theta_{12}$	0.27–0.34	0.259–0.359
$\sin^2 \theta_{23}$	0.34–0.67	0.331–0.637
$\sin^2 \theta_{13}$	0.016–0.030	0.017–0.031

with  $m_1 = \frac{1}{2}(2A + \sqrt{2}B - \sqrt{10}B)$ ,  $m_2 = \frac{1}{2}(2A + \sqrt{2}B + \sqrt{10}B)$ , and  $m_3 = -A - \sqrt{2}B + 2F$ .

For normal hierarchy (NH), the diagonal mass matrix of the light neutrinos can be written as  $m_{\text{diag}} = \text{diag}(m_1, \sqrt{m_1^2 + \Delta m_{21}^2}, \sqrt{m_1^2 + \Delta m_{31}^2})$ , whereas for inverted hierarchy (IH), it can be written as  $m_{\text{diag}} = \text{diag}(\sqrt{m_3^2 + \Delta m_{23}^2 - \Delta m_{21}^2}, \sqrt{m_3^2 + \Delta m_{23}^2}, m_3)$ . We choose two possible values of the lightest mass eigenstate  $m_1$  and  $m_3$  for normal and inverted hierarchies, respectively. First, we choose  $m_{\text{lightest}}$  as large as possible such that the sum of the absolute neutrino masses falls just below the cosmological upper bound. For normal and inverted

TABLE III. Parametrization of the neutrino mass matrix for BM.

Parameters (BM)	IH	NH	IH	NH
A	0.023946	0.015114	0.0731646	0.0741
B	0.024946	0.0141142	0.00816462	0.00409996
F	0.00027118	0.0145033	0.000163019	0.00542086
$m_3$	0.001	0.0497393	0.065	0.0858662
$m_2$	0.0492747	0.0087178	0.0815598	0.0705337
$m_1$	0.0485077	0.001	0.0810987	0.07
$\sum_i m_i$	0.0987824	0.0594571	0.22766	0.22639

TABLE IV. Parametrization of the neutrino mass matrix for TBM.

Parameters (TBM)	IH	NH	IH	NH
A	0.0487942	0.0035726	0.0812524	0.07017789
B	0.0002555	0.0025726	0.000153696	0.00017789
F	-0.023769	0.0243546	-0.00804935	0.007798948
$m_3$	0.001	0.0497092	0.065	0.0855979
$m_2$	0.0493052	0.0087178	0.0815598	0.0705337
$m_1$	0.0485387	0.001	0.0810987	0.07
$\sum_i m_i$	0.098844	0.059427	0.227657	0.226132

TABLE V. Parametrization of the neutrino mass matrix for HM.

Parameters (HM)	IH	NH	IH	NH
A	0.048699	0.00292945	0.081214	0.0701334
B	0.00023485	0.00236308	0.000141179	0.000163405
F	0.001	0.0497393	0.065	0.0858662
$m_3$	0.001	0.0497393	0.065	0.0858662
$m_2$	0.0492747	0.0087178	0.0815598	0.0705337
$m_1$	0.0485077	0.001	0.0810987	0.07
$\sum_i m_i$	0.0987824	0.0594571	0.227658	0.2261957

TABLE VI. Parametrization of the neutrino mass matrix for GRM.

Parameters (GRM)	IH	NH	IH	NH
A	0.0487197	0.00305254	0.0812261	0.0701377
B	0.0002425	0.00234835	0.000145813	0.000157545
F	0.0250314	0.0270146	0.0732162	0.0775182
$m_3$	0.001	0.047655	0.065	0.0846759
$m_2$	0.0492747	0.0084262	0.0815598	0.0704982
$m_1$	0.0485077	0.001	0.0810987	0.07
$\sum_i m_i$	0.0987824	0.057081	0.227658	0.225174

hierarchies, this turns out to be 0.07 and 0.065 eV, respectively. Then, we allow moderate hierarchy to exist between the mass eigenvalues and choose the lightest mass eigenvalue to be 0.001 eV to study the possible changes in our analysis and results. The parametrization for all these possible cases are shown in Tables III, IV, V, and VI.

For our numerical analysis, we adopt the minimal structure (14) of the type II seesaw term as

$$m_{LL}^H = \begin{pmatrix} 0 & -w & w \\ -w & w & 0 \\ w & 0 & -w \end{pmatrix}, \quad (36)$$

where  $w$  denotes the strength of perturbation coming from the type II seesaw mechanism.

We first numerically fit the leading-order  $\mu - \tau$  symmetric neutrino mass matrix (11) by taking the central values of the global fit neutrino oscillation data [6]. We also incorporate the cosmological upper bound on the sum of absolute neutrino masses [17] reported by the Planck collaboration recently. In the second step, we have to diagonalize the complete mass matrix

TABLE VII. Character table of  $A_4$ .

Class	$\chi^{(1)}$	$\chi^{(2)}$	$\chi^{(3)}$	$\chi^{(4)}$
$C_1$	1	1	1	3
$C_2$	1	$\omega$	$\omega^2$	0
$C_3$	1	$\omega^2$	$\omega$	0
$C_4$	1	1	1	-1

$$m_\nu = m_\nu^{(0)} + m_\nu^{(\text{pert})} = m_\nu^I + m_\nu^{II},$$

and as a result, there is a corresponding mixing matrix for which the elements are related to the parameters of the model plus the strength of the type II perturbation term.

After fitting the type I seesaw contribution to the neutrino mass with experimental data, we introduce the type II seesaw contribution as a perturbation to the  $\mu - \tau$  symmetric neutrino mass matrix. The strength of the type II seesaw perturbation in order to generate the correct value of nonzero  $\theta_{13}$  can be seen from Figs. 5–7, and 8. We also calculate other neutrino parameters by varying the type II seesaw strength and show our results as a function of  $\sin^2 \theta_{13}$  in Figs. 9–11, and 12 for BM mixing; Figs. 13–15, and 16 for TBM mixing; Figs. 17–19, and 20 for Hexagonal mixing; and Figs. 21, 22, 23, and 24 for GR mixing. We also calculate the sum of the absolute neutrino masses  $\sum_i |m_i|$  to check whether it lies below the Planck upper bound. Finally, we calculate the effective neutrino mass  $m_{ee} = |\sum_i U_{ei}^2 m_i|$ , which can play a great role in neutrinoless double beta decay. These are shown as a function of  $\sin^2 \theta_{13}$  in Figs. 25–31, and 32.

To calculate the baryon asymmetry, we first have to make a choice of the diagonal Dirac neutrino mass matrix  $m_{LR}^d$ . The most natural choice is to take  $m_{LR}^d$  to be the same as the diagonal charged lepton mass matrix. We check this particular case and find that this corresponds to a three-flavor leptogenesis scenario, and for all values of the Dirac  $CP$  phase  $\delta$ , the resulting baryon asymmetry falls far outside the observed range. As discussed in our earlier work [23], here also we assume the parametric form of  $m_{LR}^d$

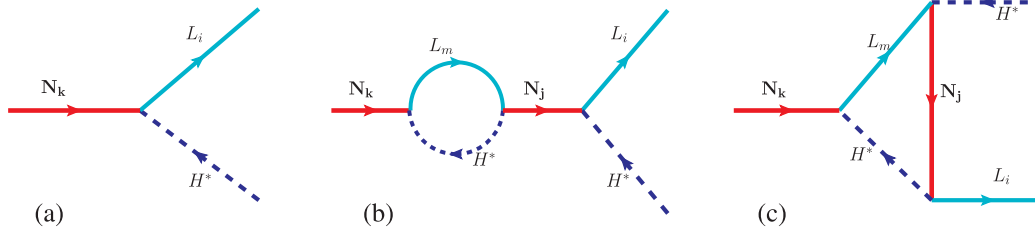


FIG. 1 (color online). Right-handed neutrino decay.

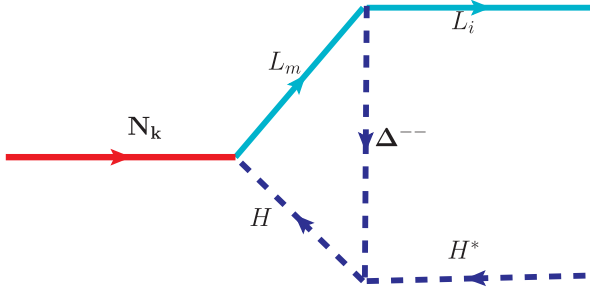


FIG. 2 (color online). Right-handed neutrino decay.

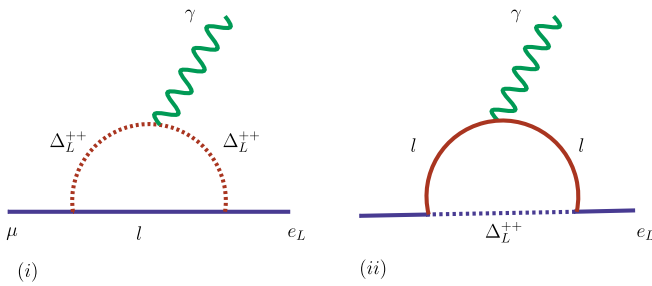


FIG. 3 (color online). Relevant Feynman diagram for  $\mu \rightarrow e\gamma$  due to Higgs triplet exchange.

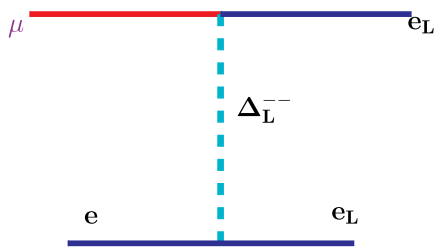


FIG. 4 (color online). Relevant Feynman diagram for  $\mu \rightarrow eee$  due to Higgs triplet exchange.

as given in (28) and choose the integers  $(m, n)$  in such a way that the lightest right-handed neutrino mass falls either in the one-flavor or two-flavor or three-flavor regime. We take  $m_f = 82.43$  GeV and find that the choice  $(m, n) = (1, 1)$  keeps the lightest right-handed neutrino in the one-flavor regime, that is,  $M_1 >$

$10^{12}$  GeV. For  $(m, n) = (3, 1)$ , the lightest right-handed neutrino mass is in the range  $10^9 < M_1 < 10^{12}$  GeV, which corresponds to the two-flavor regime of leptogenesis as discussed in the previous section. Similarly, to keep the lightest right-handed neutrino mass below  $10^9$  GeV, the three-flavor regime, we take  $(m, n)$  as  $(5, 3)$  in the Dirac neutrino mass matrix (28). The values of the type II seesaw strength  $w$  and corresponding neutrino neutrino mixing angles used in the calculation of leptogenesis are shown in Table VIII. The results for final baryon asymmetry are shown in Figs. 33 and 34 for BM, TBM, and HM models. Since GRM models do not give rise to correct neutrino parameters, we do not calculate the baryon asymmetry for that case.

### VIII. RESULTS AND CONCLUSION

We have studied the possibility of generating nonzero  $\theta_{13}$  by perturbing the  $\mu - \tau$  symmetric neutrino mass matrix using the type II seesaw. The leading-order  $\mu - \tau$  symmetric mass matrix originating from the type I seesaw can be of four different types, bimaximal, tribimaximal, hexagonal, and golden ratio mixing, which differ by the solar mixing angle they predict. All these four different types of mixing predict  $\theta_{23} = 45^\circ$  and  $\theta_{13} = 0$ . We use a minimal  $\mu - \tau$  symmetry breaking form of the type II seesaw mass matrix to perturb the type I seesaw mass matrix and determine the strength of the type II seesaw term in order to generate nonzero  $\theta_{13}$  in the correct  $3\sigma$  range. We find that, except in the case of golden ratio mixing with inverted hierarchy and  $m_3 = 0.001$  eV, all other cases under consideration give rise to correct values of  $\theta_{13}$  as can be seen from Figs. 5–7, and 8. We then calculate other neutrino parameters as we vary the type II seesaw strength and show their variations as a function of  $\sin^2 \theta_{13}$ . We find that bimaximal mixing with inverted hierarchy, tribimaximal mixing with both normal and inverted hierarchies, and hexagonal mixing with normal hierarchy can give rise to correct values of neutrino parameters as well as baryon asymmetry. The golden ratio mixing is disfavored in our framework for both types of neutrino mass hierarchies. We have estimated branching ratios for LFV decays like  $\mu \rightarrow e + \gamma$  and  $\mu \rightarrow 3e$  due to the presence of a few hundreds of GeV mass scale doubly charged scalar triplet Higgs. The estimated

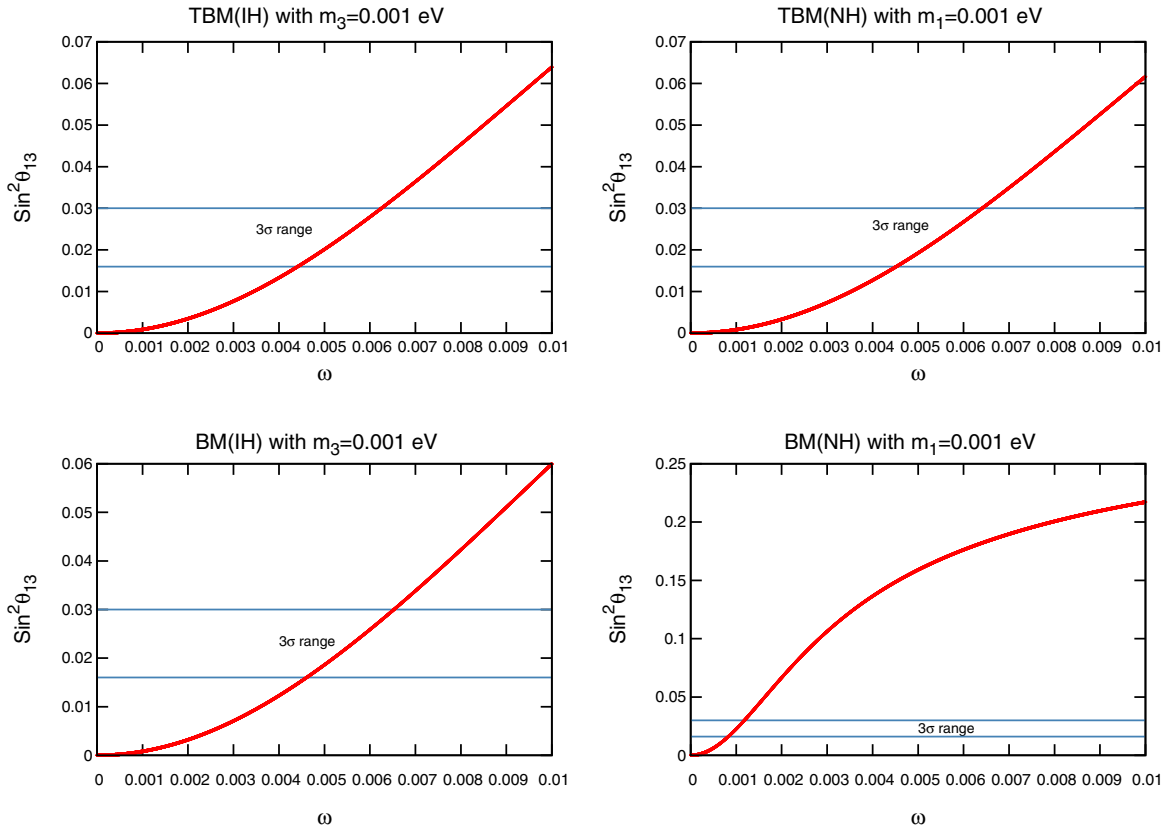


FIG. 5 (color online). Variation of  $\sin^2 \theta_{13}$  with type II seesaw strength  $w$  for BM and TBM with  $m_1(m_3) = 0.07(0.065)$  eV.

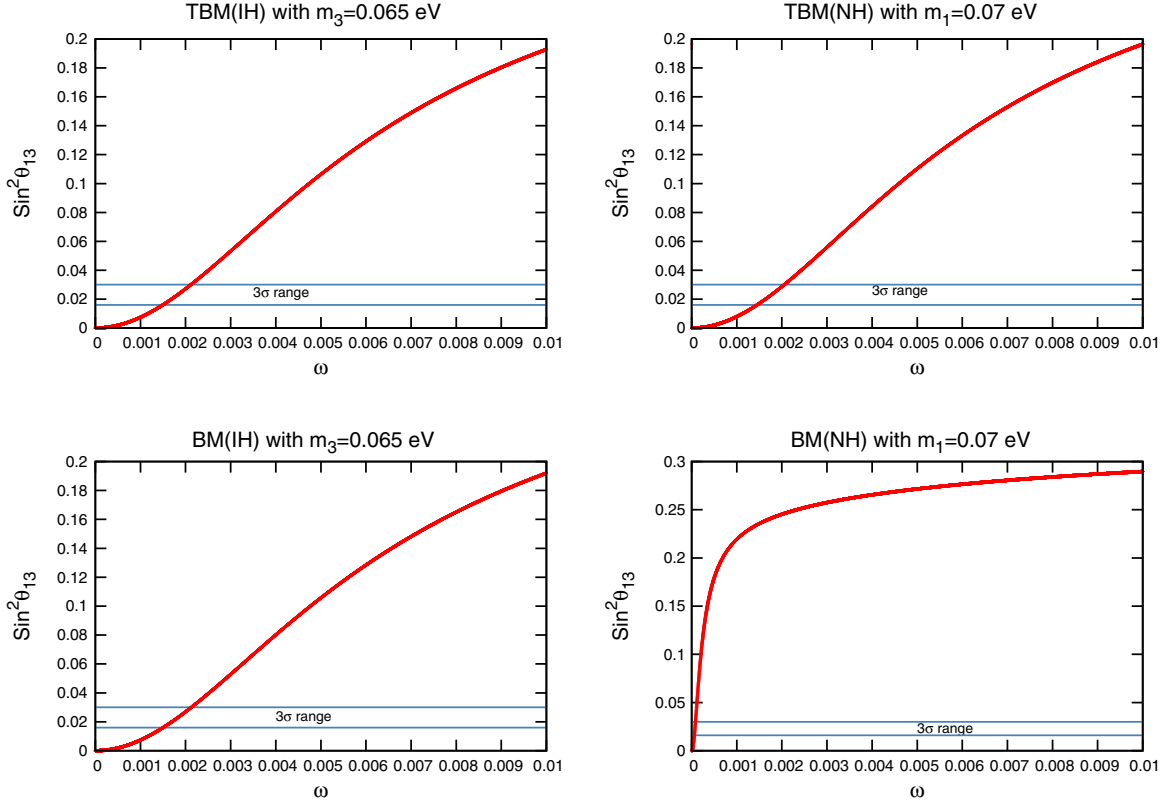


FIG. 6 (color online).  $\sin^2 \theta_{13}$  with type II seesaw strength  $w$  for BM and TBM with  $m_1(m_3) = 0.07(0.065)$  eV.



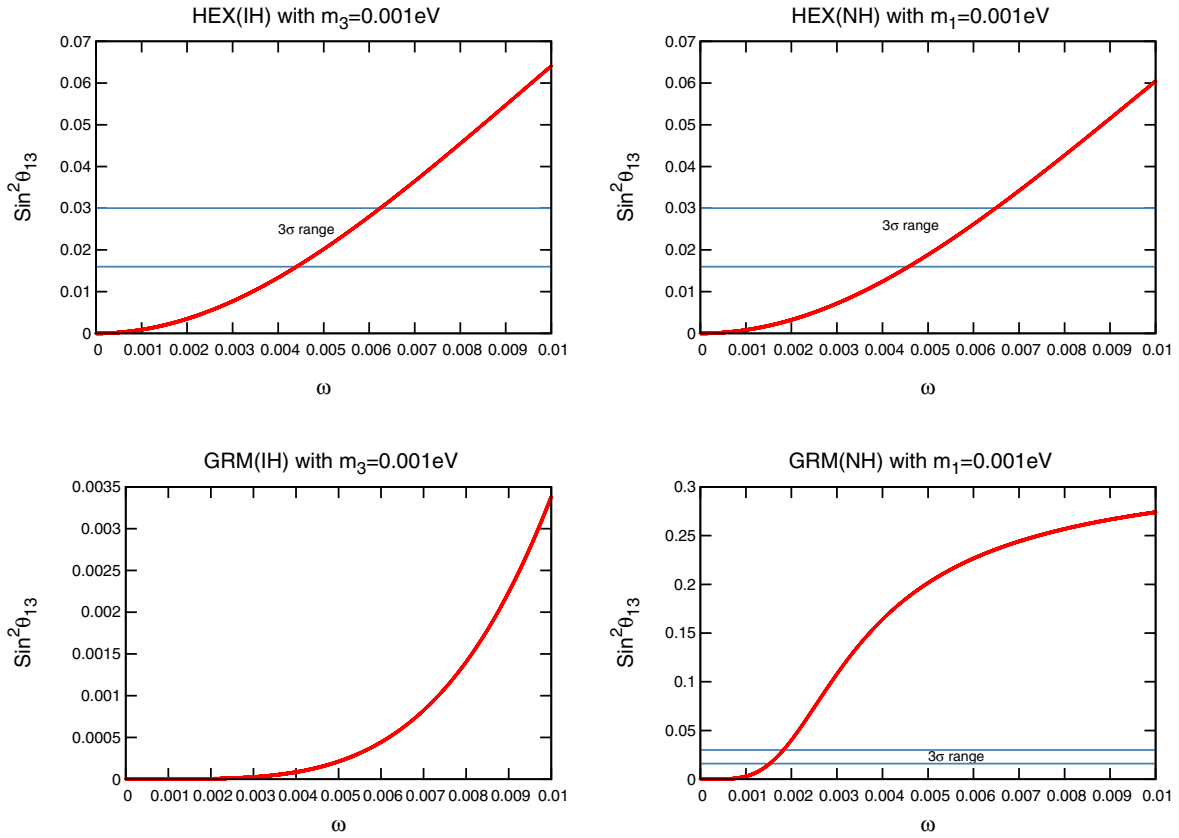


FIG. 7 (color online).  $\sin^2 \theta_{13}$  with type II seesaw strength  $w$  for HM and GRM with  $m_1(m_3) = 0.001$  eV.

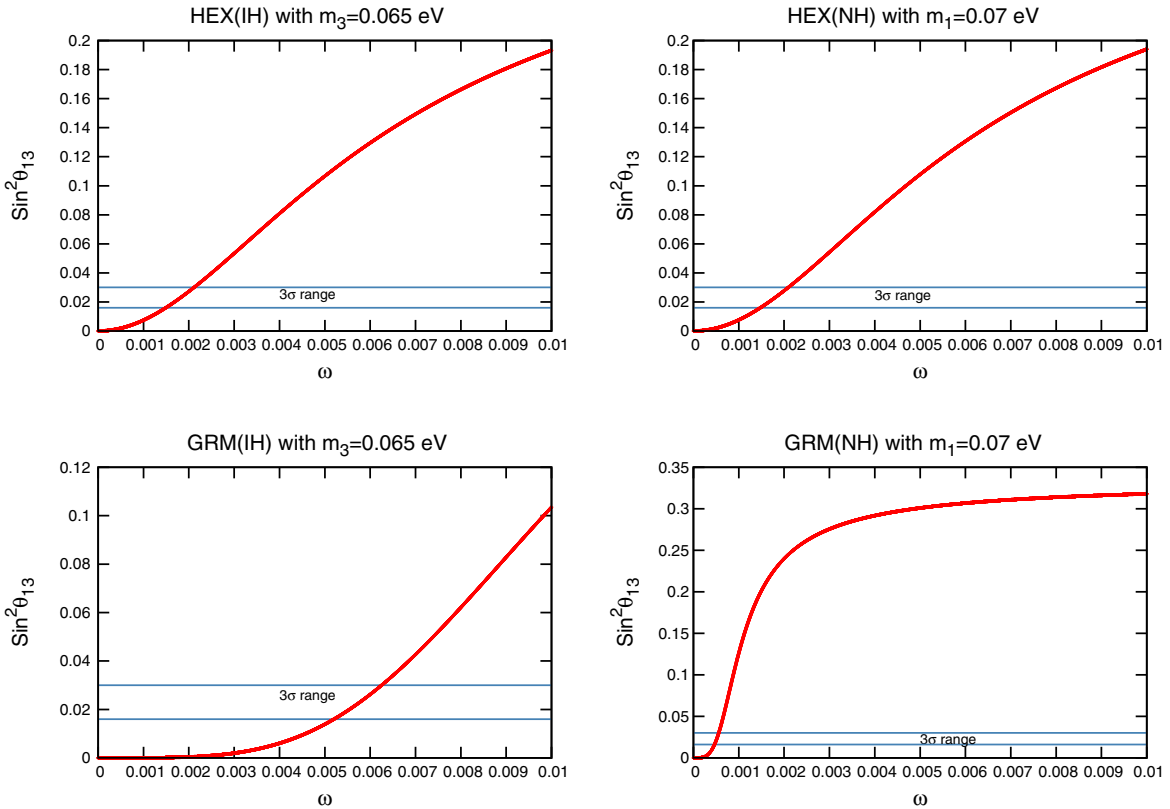


FIG. 8 (color online).  $\sin^2 \theta_{13}$  with type II seesaw strength  $w$  for HM and GRM with  $m_1(m_3) = 0.07(0.065)$  eV.

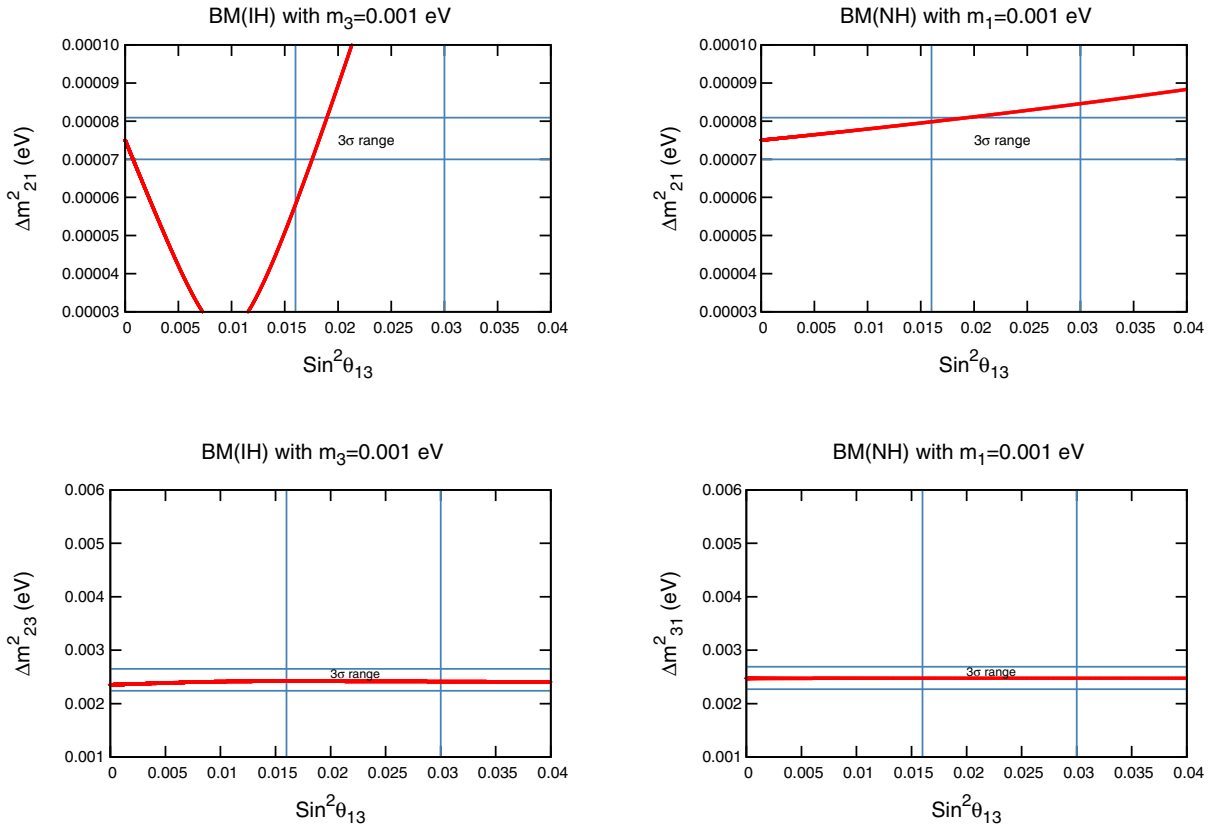


FIG. 9 (color online).  $\Delta m^2_{21}$ ,  $\Delta m^2_{23}$ , and  $\Delta m^2_{31}$  with  $\sin^2 \theta_{13}$  for BM with  $m_1(m_3) = 0.001$  eV.

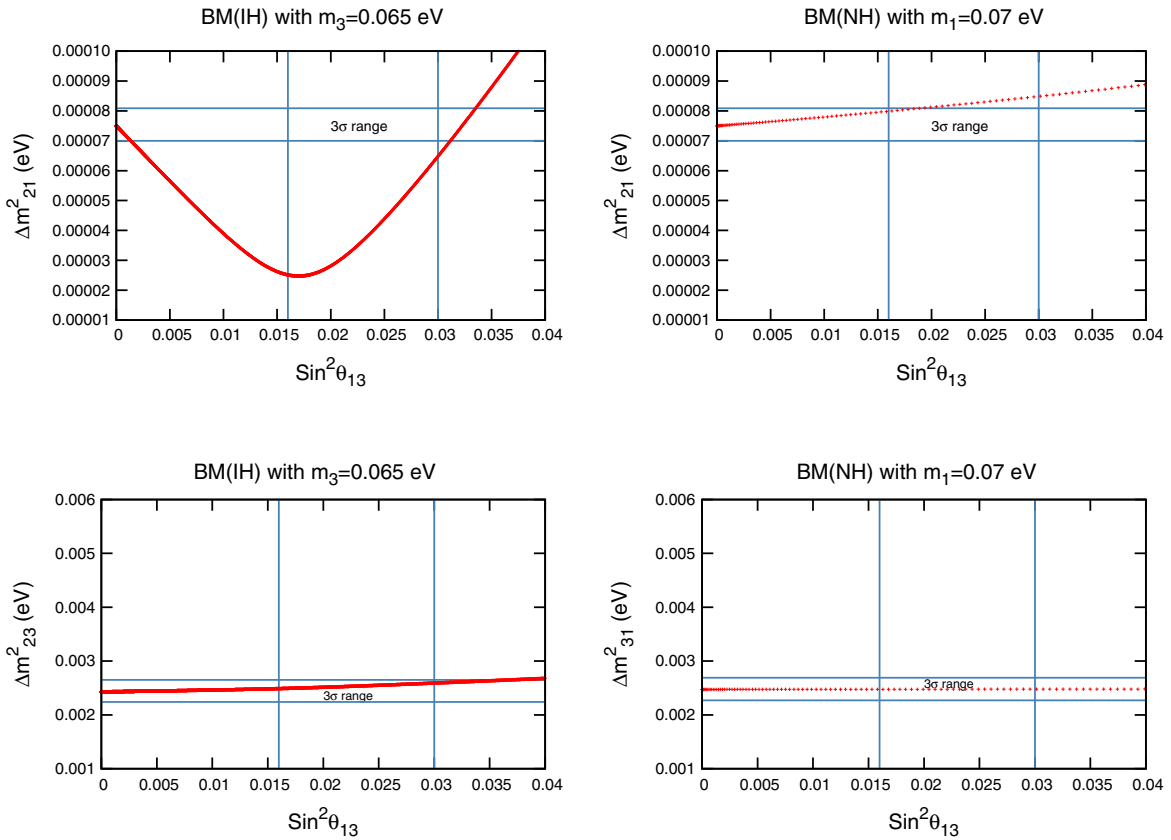


FIG. 10 (color online).  $\Delta m^2_{21}$ ,  $\Delta m^2_{23}$ , and  $\Delta m^2_{31}$  with  $\sin^2 \theta_{13}$  for BM with  $m_1(m_3) = 0.07(0.065)$  eV.

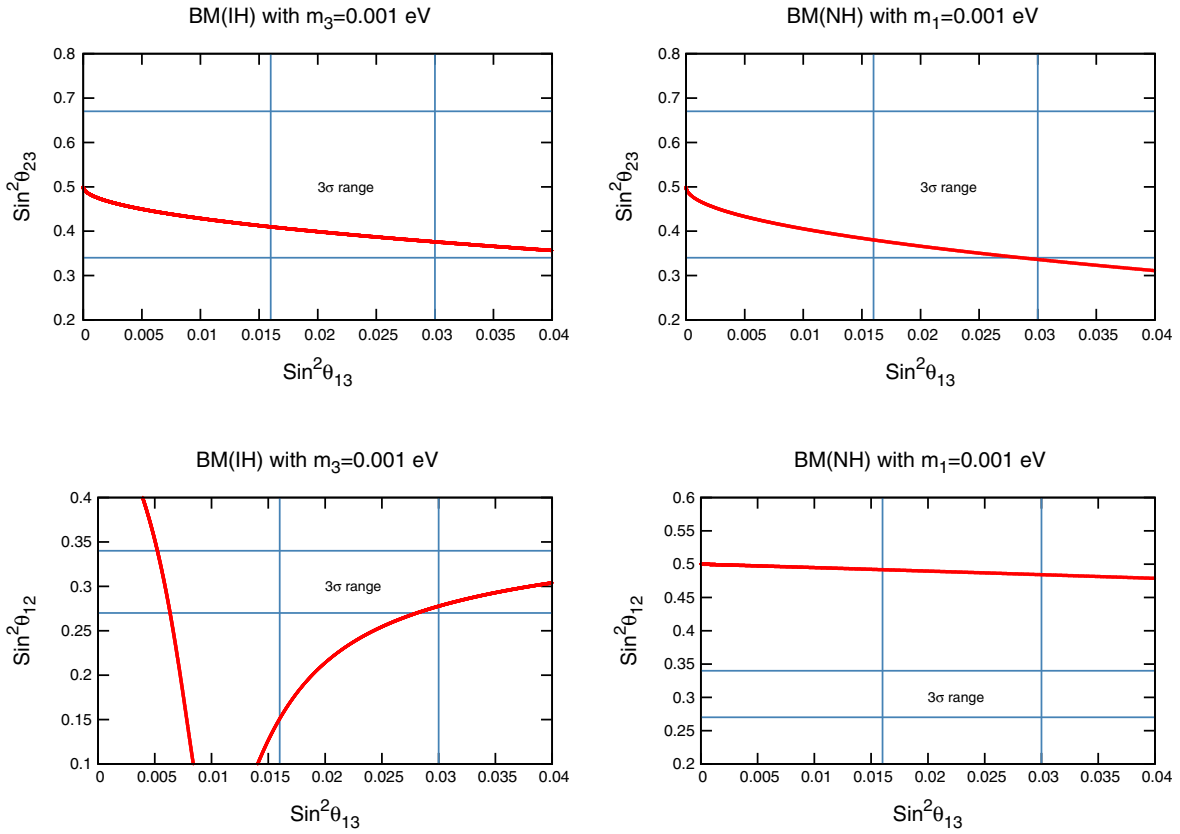


FIG. 11 (color online).  $\sin^2 \theta_{23}$  and  $\sin^2 \theta_{12}$  with  $\sin^2 \theta_{13}$  for BM with  $m_1(m_3) = 0.001$  eV.

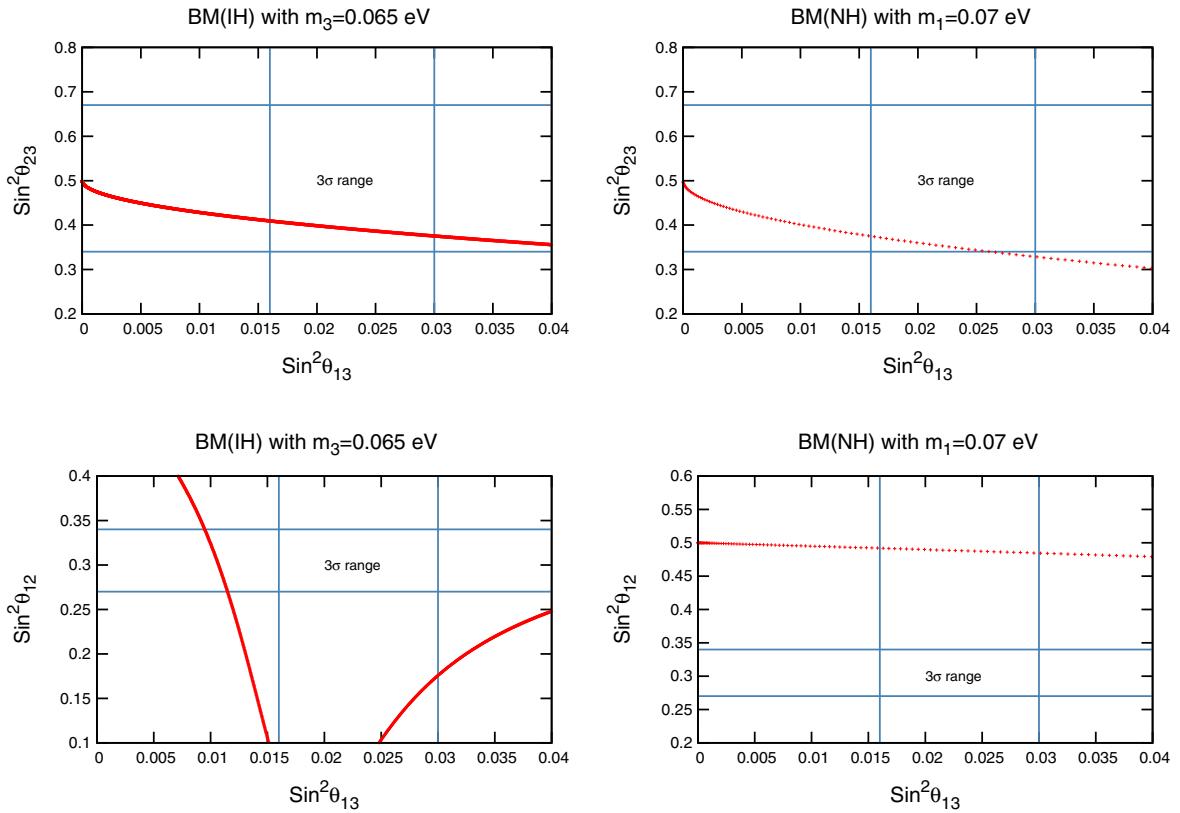


FIG. 12 (color online).  $\sin^2 \theta_{23}$  and  $\sin^2 \theta_{12}$  with  $\sin^2 \theta_{13}$  for BM with  $m_1(m_3) = 0.07(0.065)$  eV.

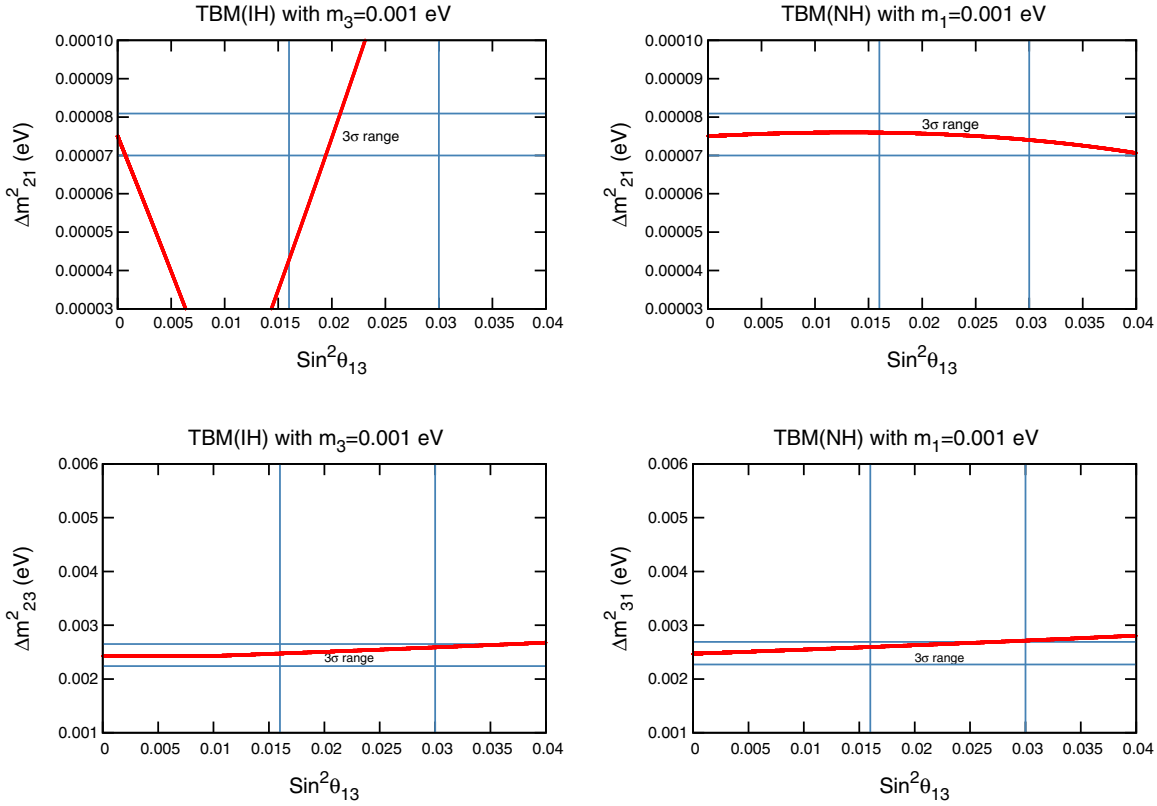


FIG. 13 (color online).  $\Delta m^2_{21}$ ,  $\Delta m^2_{23}$ , and  $\Delta m^2_{31}$  with  $\sin^2 \theta_{13}$  for TBM with  $m_1(m_3) = 0.001$  eV.

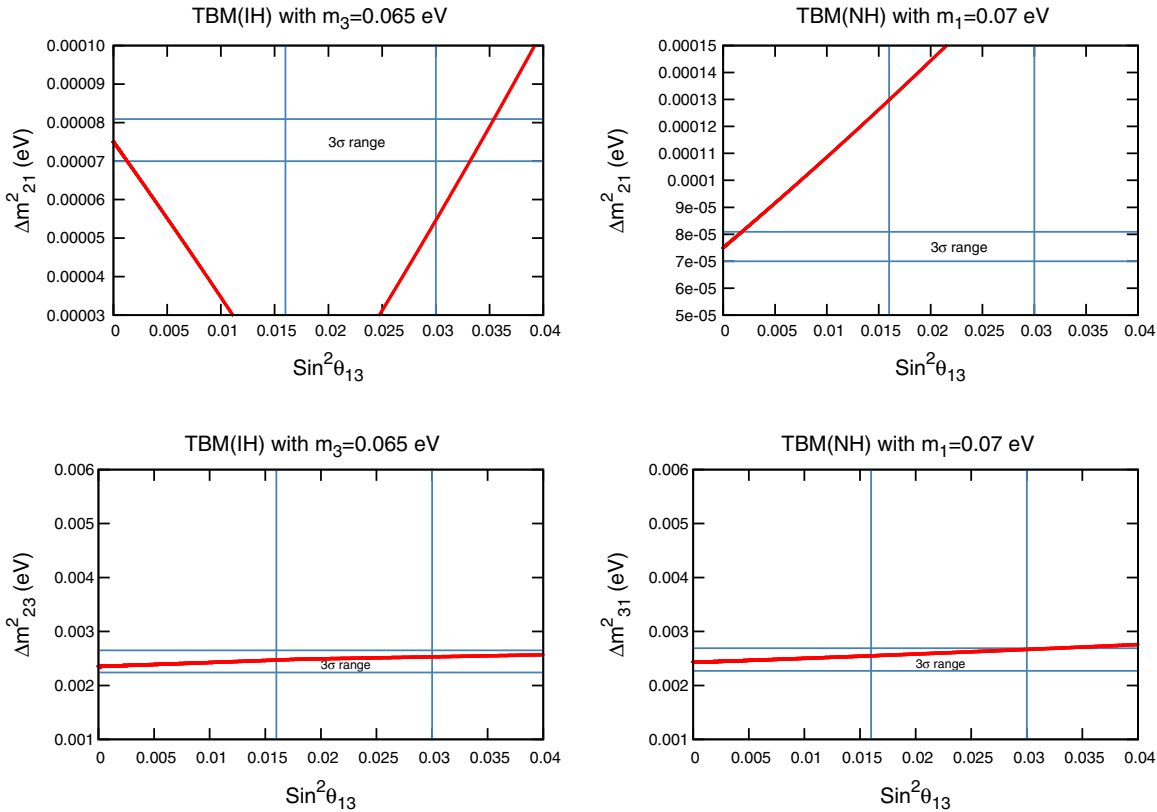


FIG. 14 (color online).  $\Delta m^2_{21}$ ,  $\Delta m^2_{23}$ , and  $\Delta m^2_{31}$  with  $\sin^2 \theta_{13}$  for TBM with  $m_1(m_3) = 0.07(0.065)$  eV.



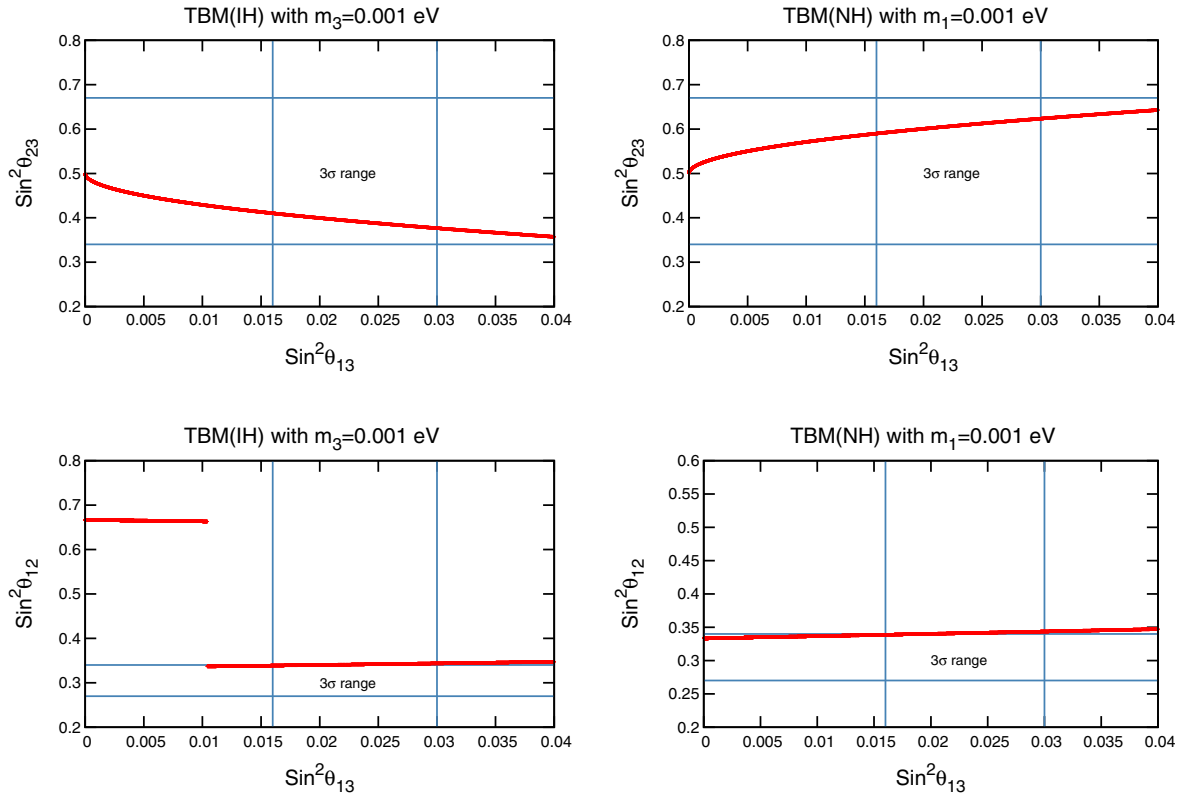


FIG. 15 (color online).  $\sin^2 \theta_{23}$ , and  $\sin^2 \theta_{12}$  with  $\sin^2 \theta_{13}$  for TBM with  $m_1(m_3) = 0.001$  eV.

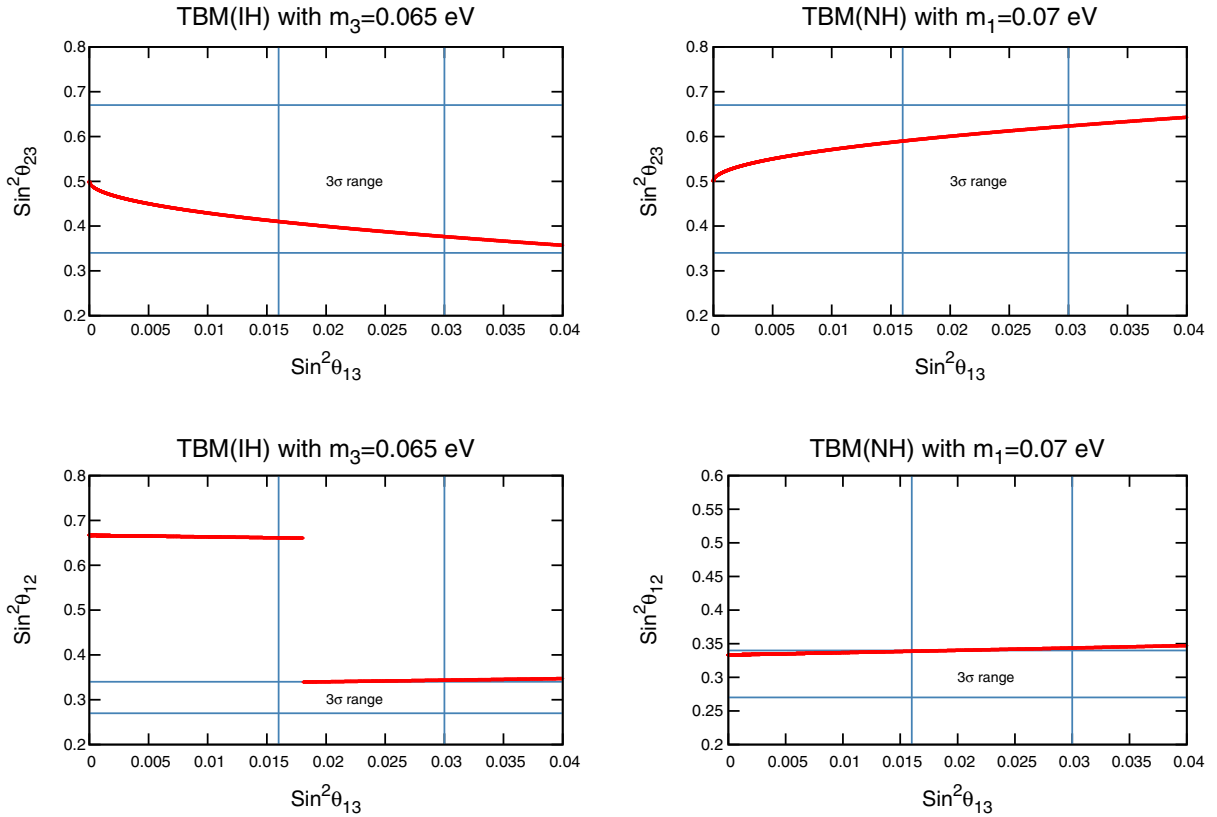


FIG. 16 (color online).  $\sin^2 \theta_{23}$ , and  $\sin^2 \theta_{12}$  with  $\sin^2 \theta_{13}$  for TBM with  $m_1(m_3) = 0.07(0.065)$  eV.

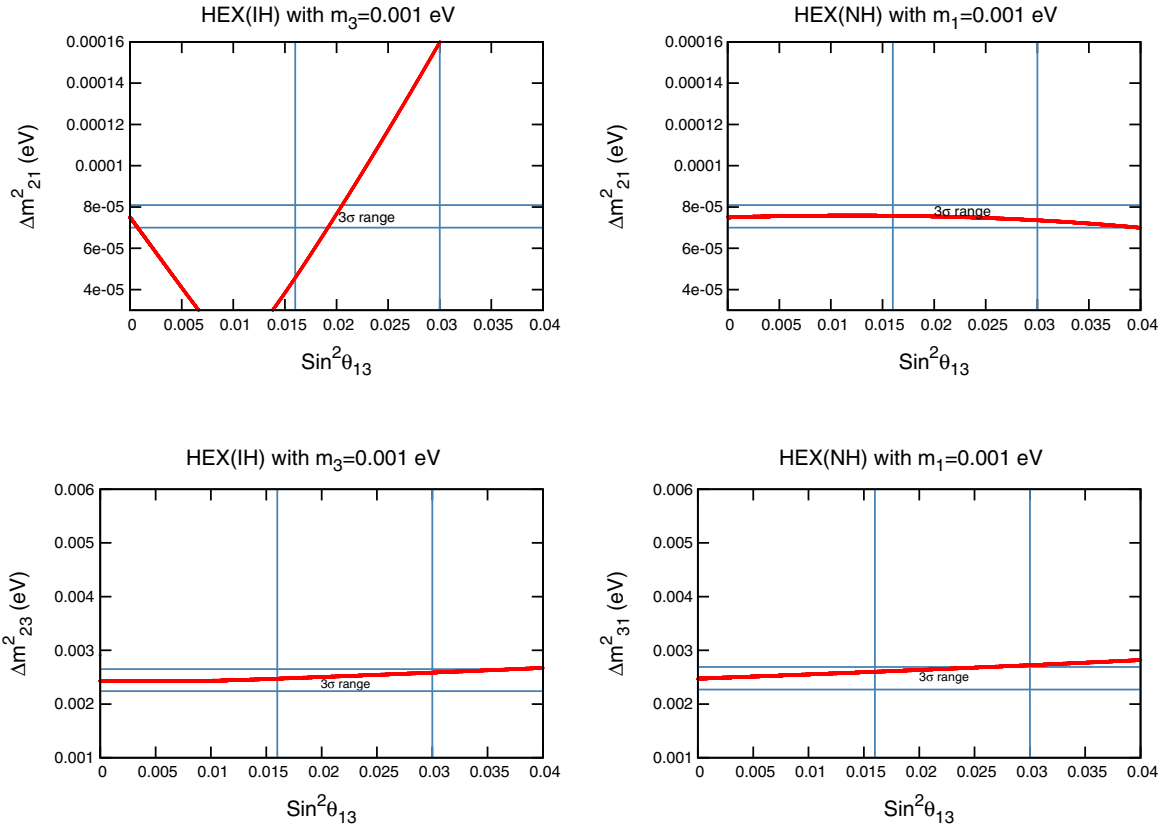


FIG. 17 (color online).  $\Delta m^2_{21}$ ,  $\Delta m^2_{23}$ , and  $\Delta m^2_{31}$  with  $\sin^2 \theta_{13}$  for HM with  $m_1(m_3) = 0.001$  eV.

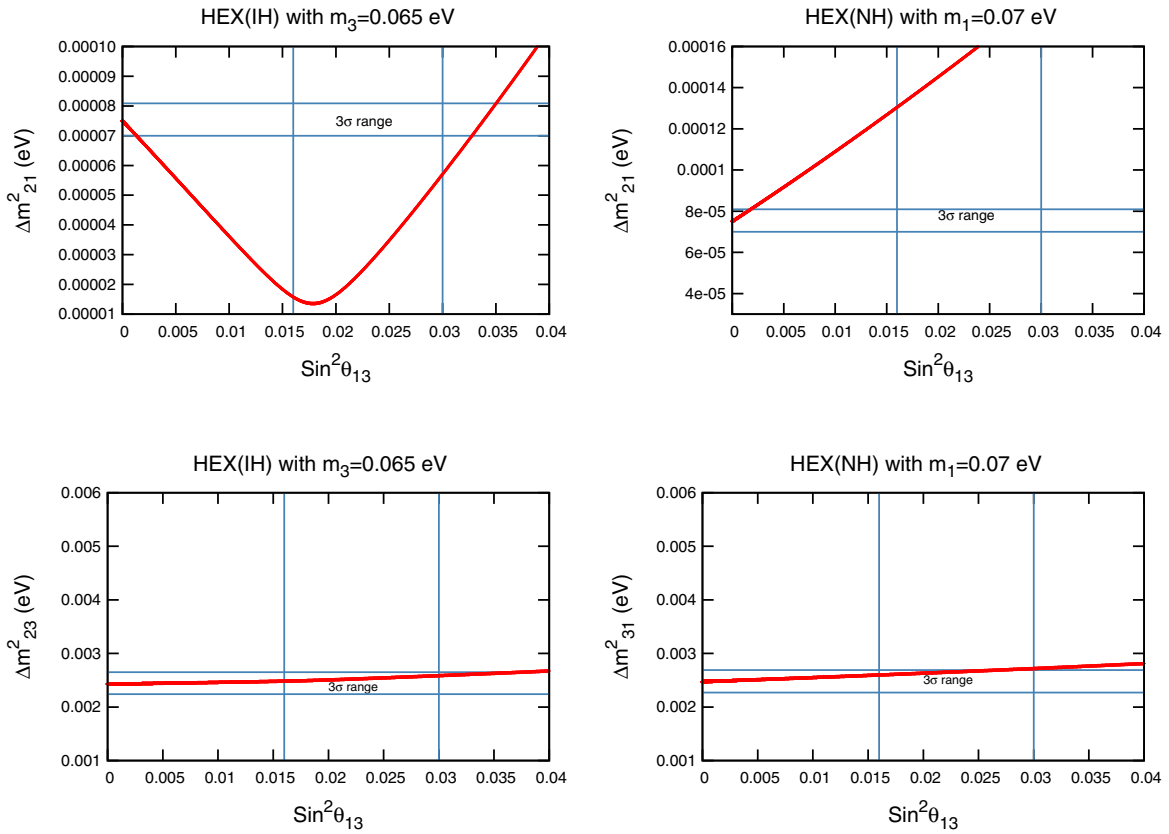


FIG. 18 (color online).  $\Delta m^2_{21}$ ,  $\Delta m^2_{23}$ , and  $\Delta m^2_{31}$  with  $\sin^2 \theta_{13}$  for HM with  $m_1(m_3) = 0.07(0.065)$  eV.

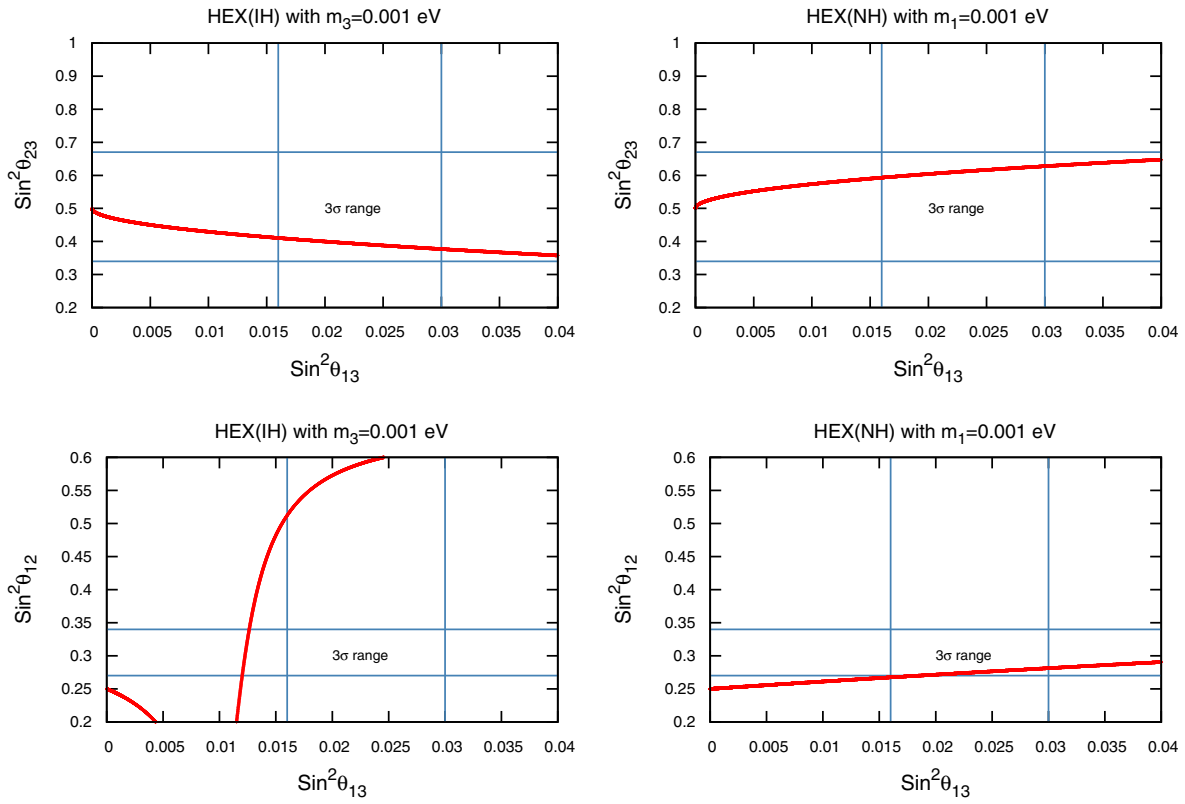


FIG. 19 (color online).  $\sin^2 \theta_{23}$  and  $\sin^2 \theta_{12}$  with  $\sin^2 \theta_{13}$  for HM with  $m_1(m_3) = 0.001$  eV.

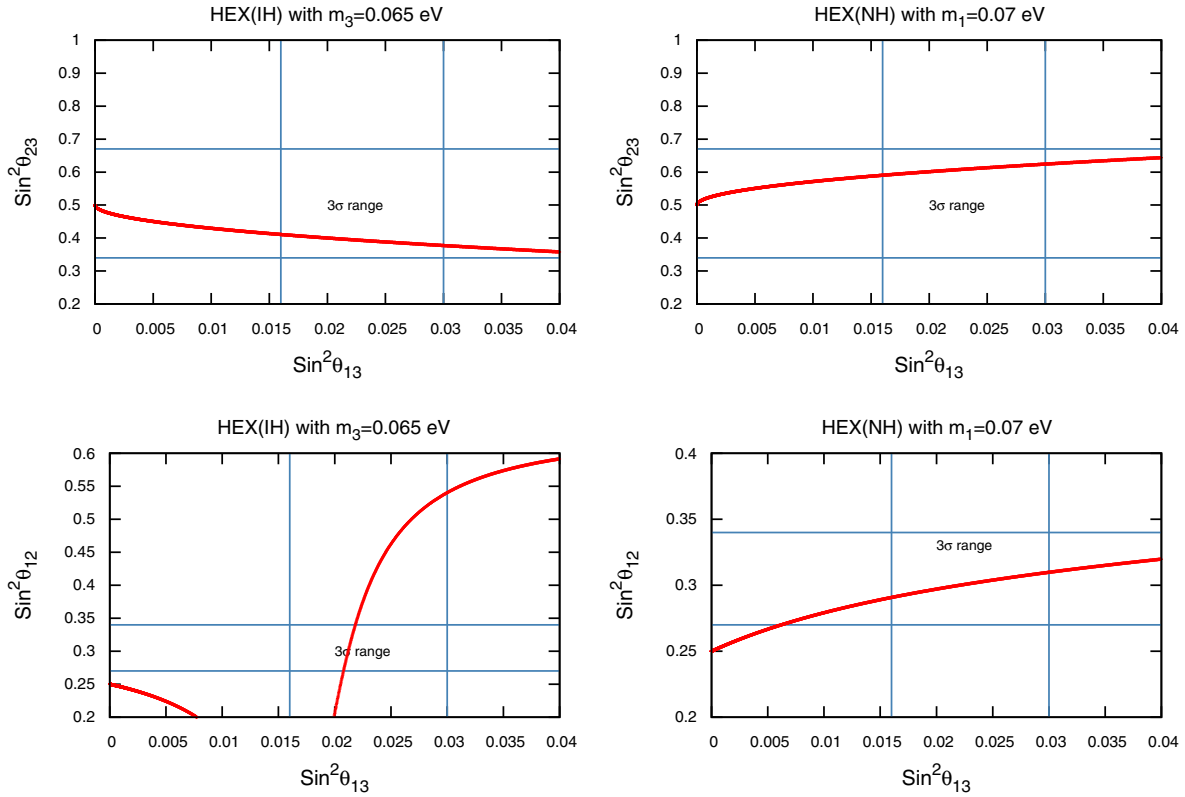


FIG. 20 (color online).  $\sin^2 \theta_{23}$  and  $\sin^2 \theta_{12}$  with  $\sin^2 \theta_{13}$  for HM with  $m_1(m_3) = 0.07(0.065)$  eV.

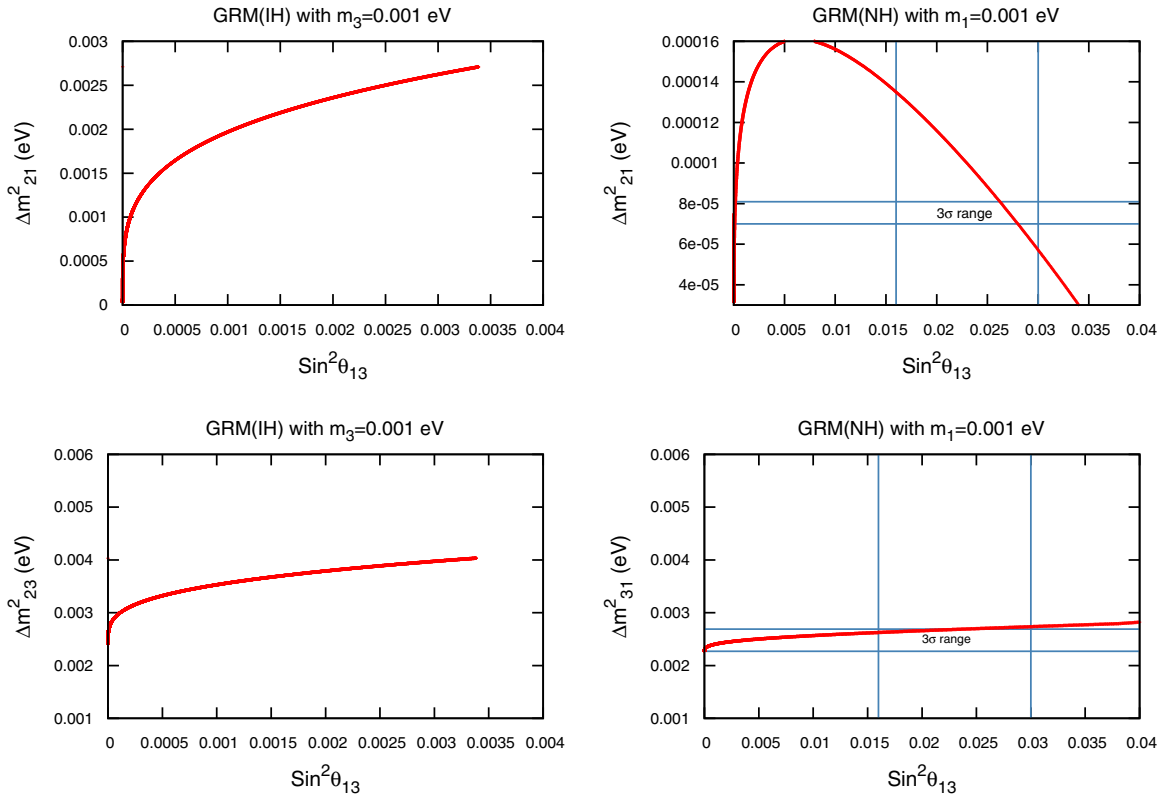


FIG. 21 (color online).  $\Delta m^2_{21}$ ,  $\Delta m^2_{23}$ , and  $\Delta m^2_{31}$  with  $\sin^2 \theta_{13}$  for GRM with  $m_1(m_3) = 0.001$  eV.

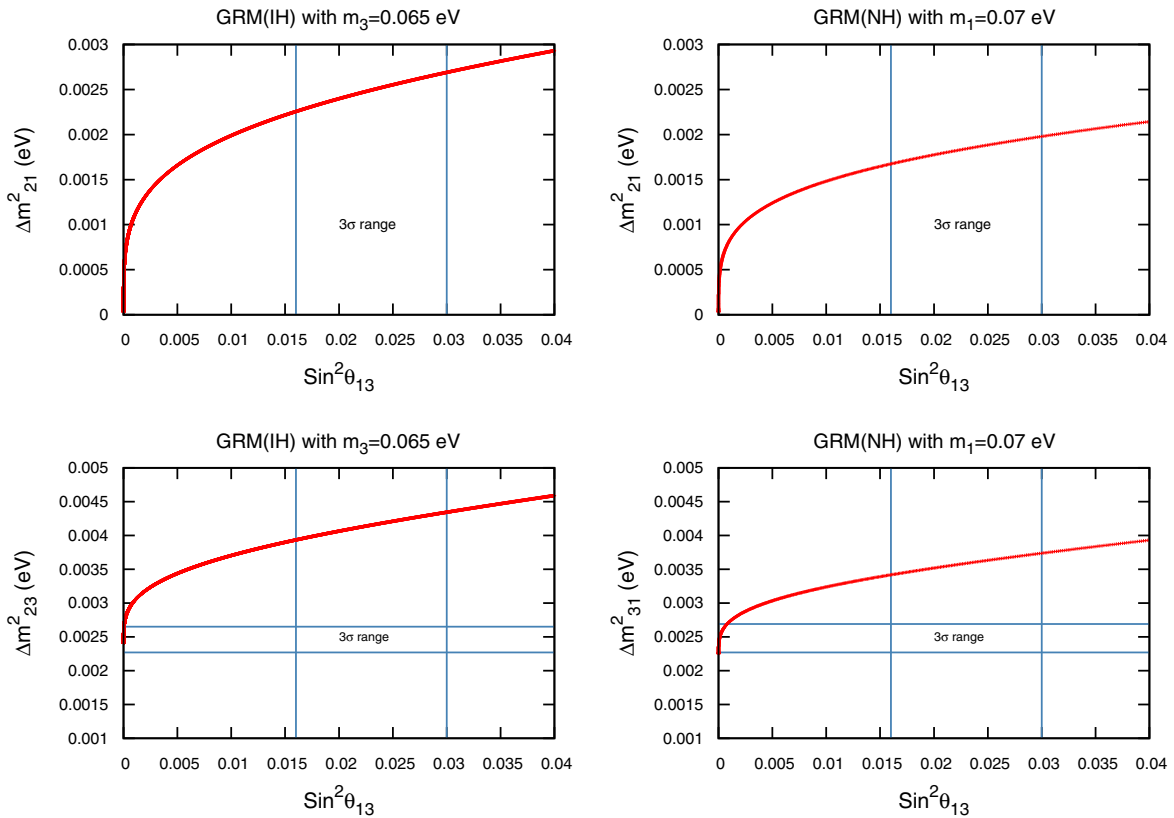


FIG. 22 (color online).  $\Delta m^2_{21}$ ,  $\Delta m^2_{23}$ , and  $\Delta m^2_{31}$  with  $\sin^2 \theta_{13}$  for GRM with  $m_1(m_3) = 0.07(0.065)$  eV.



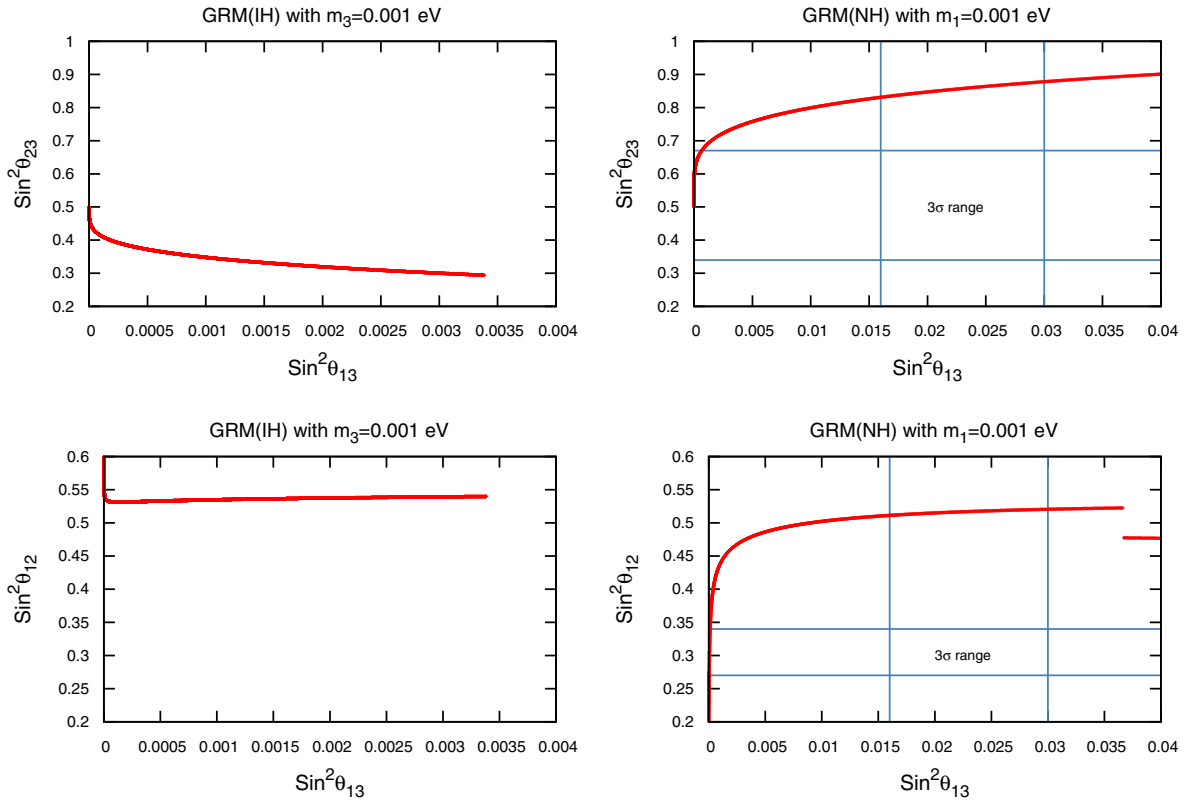


FIG. 23 (color online).  $\sin^2 \theta_{23}$  and  $\sin^2 \theta_{12}$  with  $\sin^2 \theta_{13}$  for GRM with  $m_1(m_3) = 0.001$  eV.

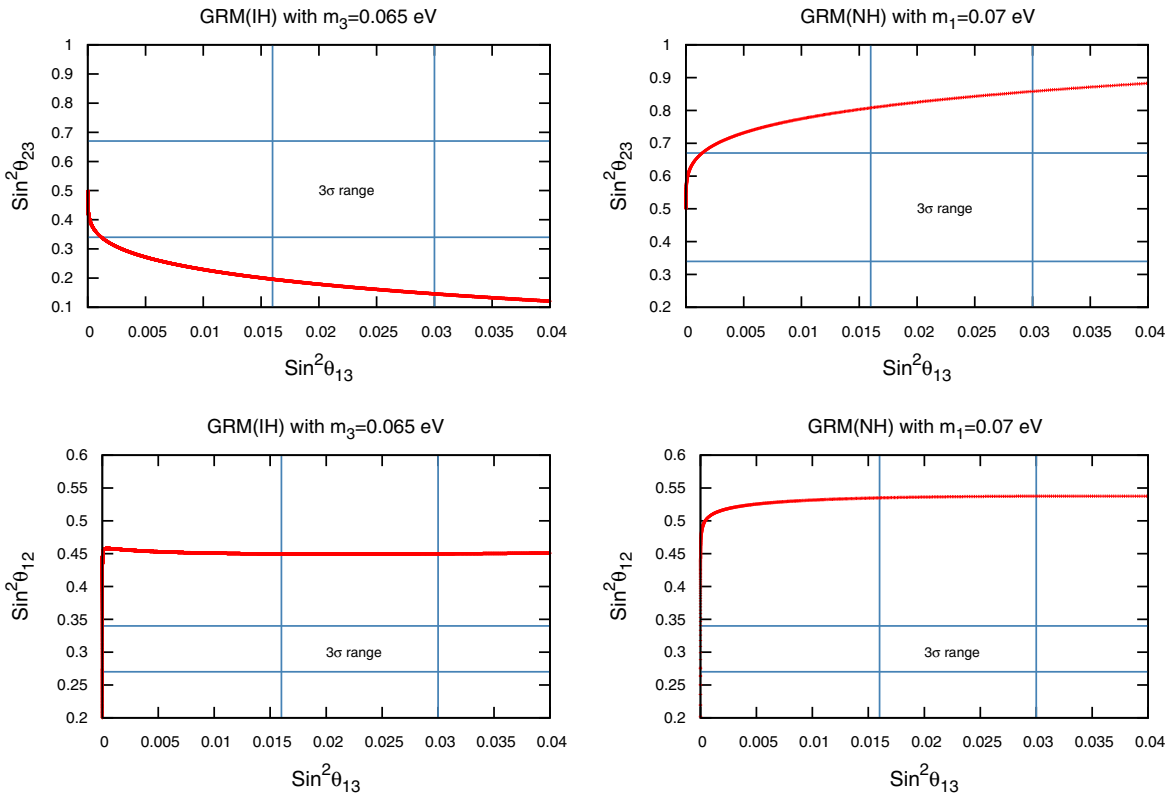


FIG. 24 (color online).  $\sin^2 \theta_{23}$  and  $\sin^2 \theta_{12}$  with  $\sin^2 \theta_{13}$  for GRM with  $m_1(m_3) = 0.07(0.065)$  eV.

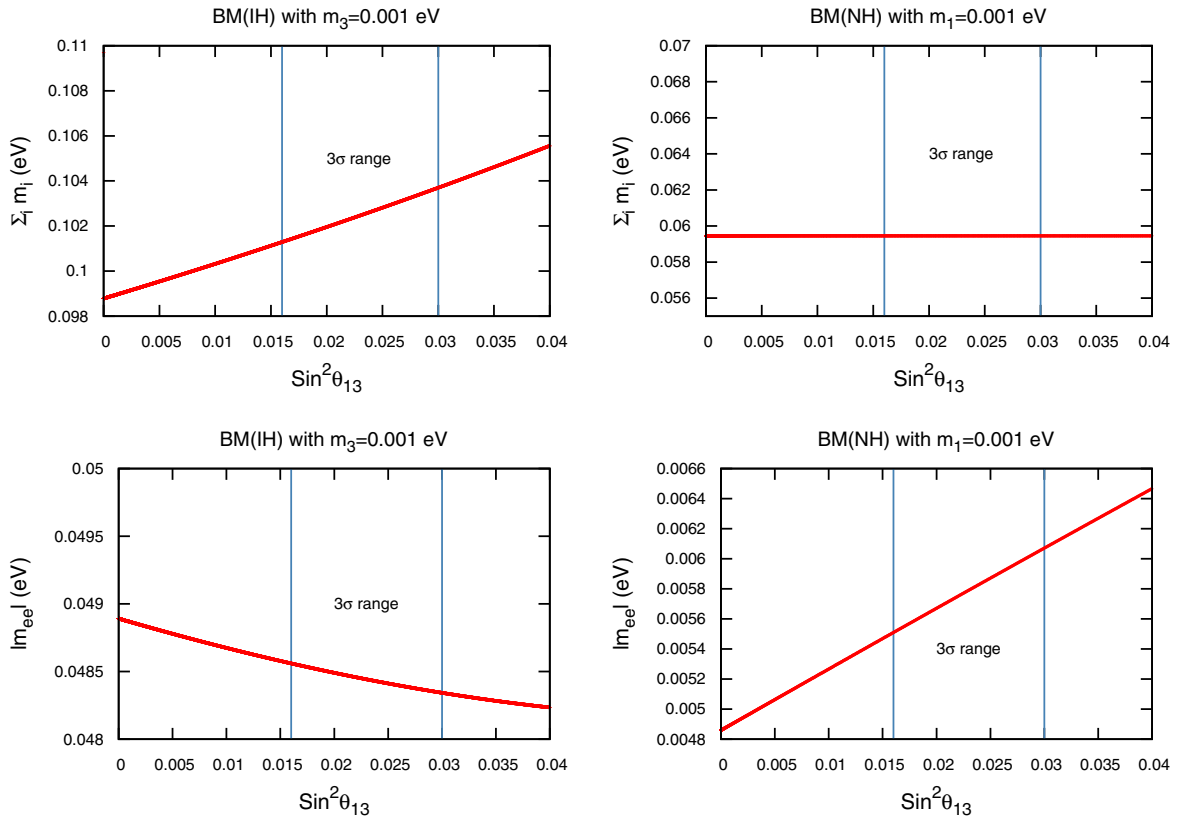


FIG. 25 (color online).  $\sum_i |m_i|$  and  $|m_{ee}|$  with  $\sin^2 \theta_{13}$  for BM with  $m_1(m_3) = 0.001$  eV.

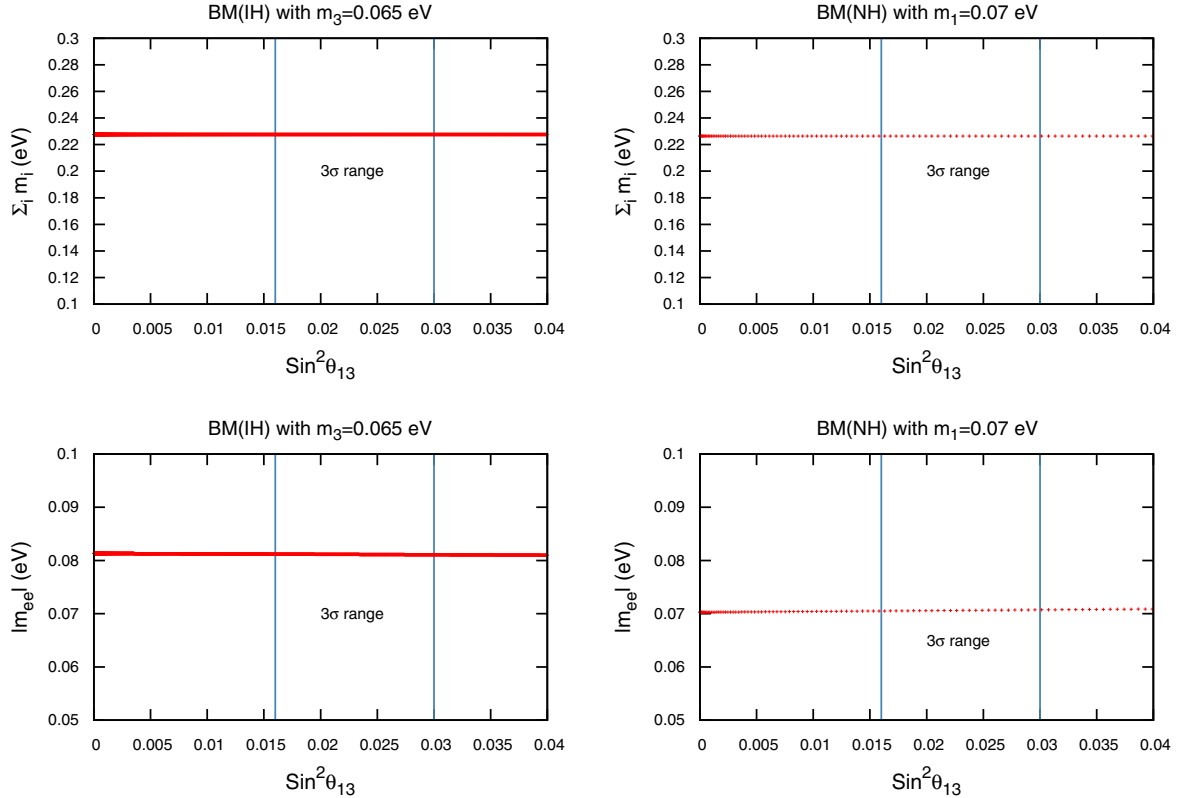


FIG. 26 (color online).  $\sum_i |m_i|$  and  $|m_{ee}|$  with  $\sin^2 \theta_{13}$  for BM with  $m_1(m_3) = 0.07(0.065)$  eV.

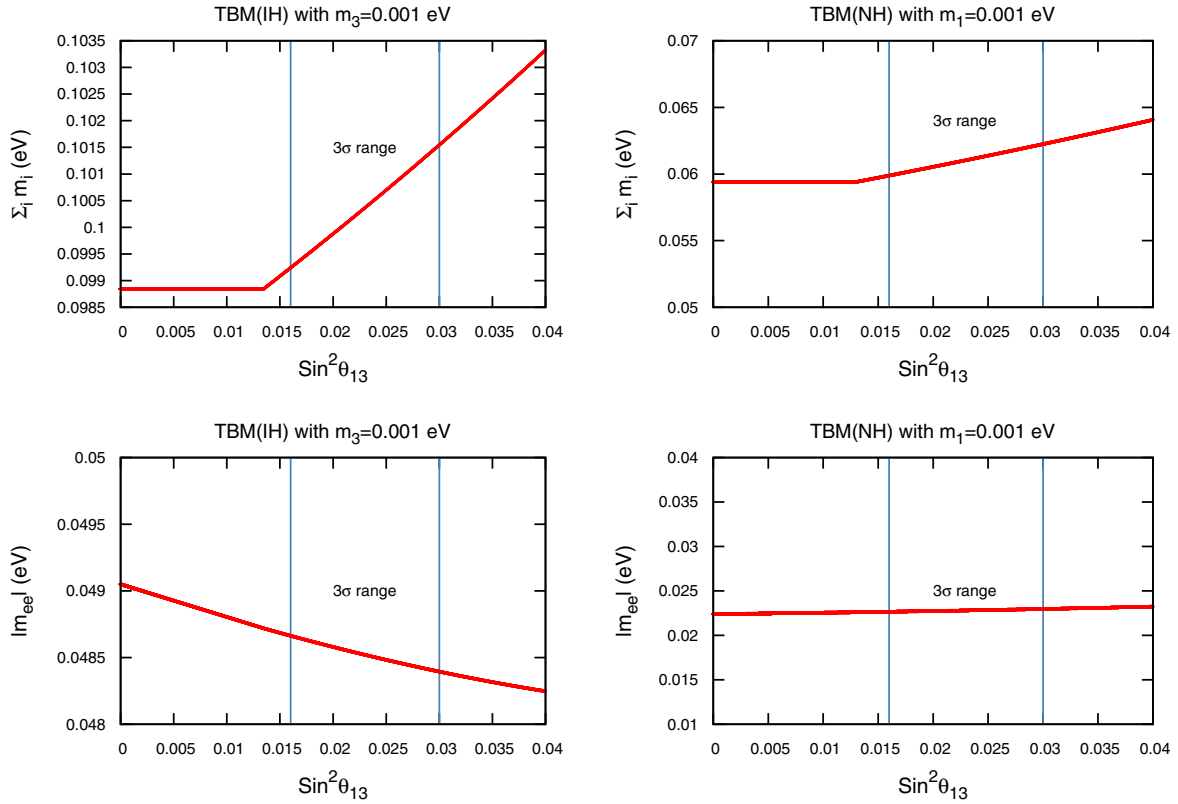


FIG. 27 (color online).  $\sum_i |m_i|$  and  $|m_{ee}|$  with  $\sin^2 \theta_{13}$  for TBM with  $m_1(m_3) = 0.001$  eV.

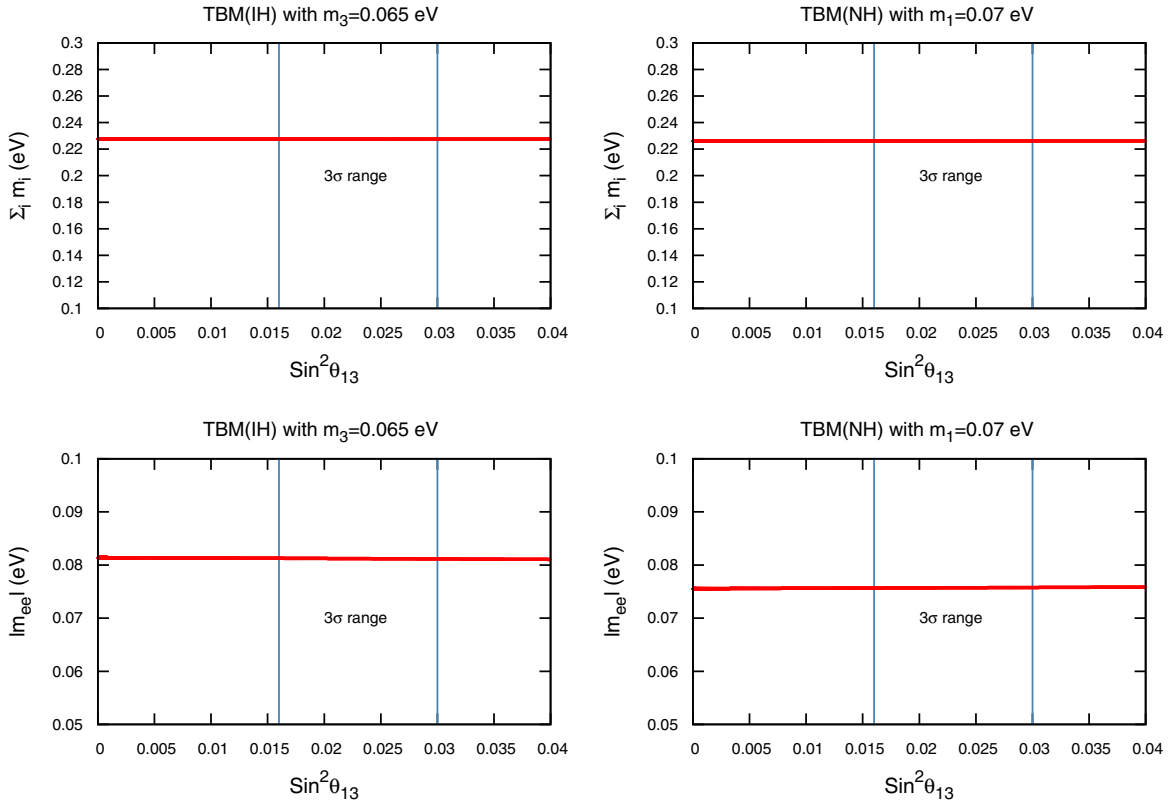


FIG. 28 (color online).  $\sum_i |m_i|$  and  $|m_{ee}|$  with  $\sin^2 \theta_{13}$  for TBM with  $m_1(m_3) = 0.07(0.065)$  eV.

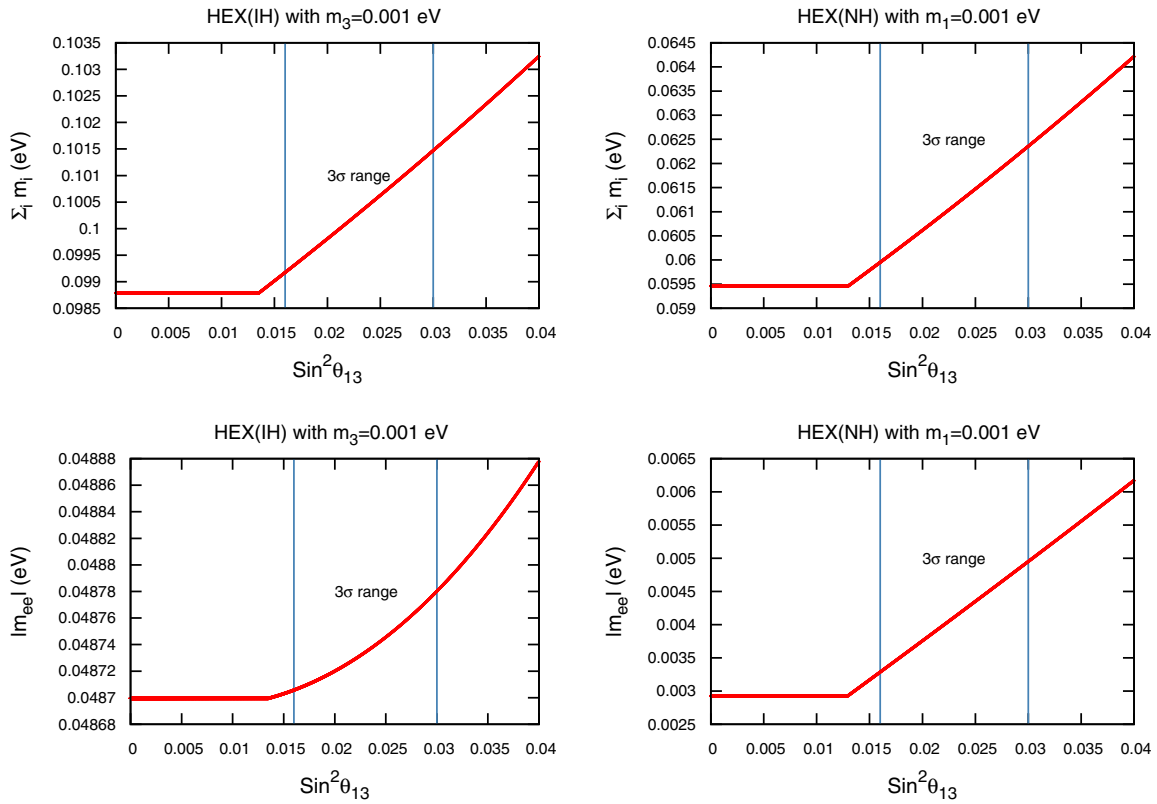


FIG. 29 (color online).  $\sum_i |m_i|$  and  $|m_{ee}|$  with  $\sin^2 \theta_{13}$  for HM with  $m_1(m_3) = 0.001$  eV.

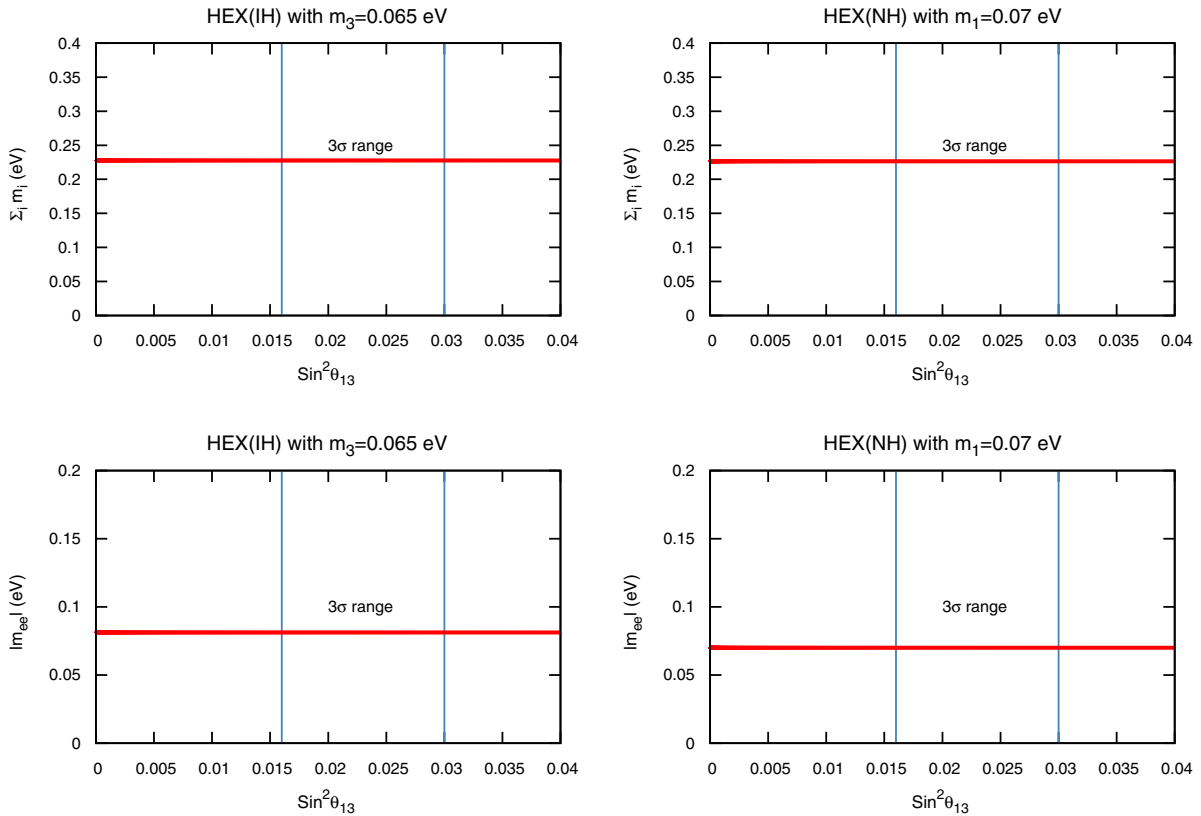


FIG. 30 (color online).  $\sum_i |m_i|$  and  $|m_{ee}|$  with  $\sin^2 \theta_{13}$  for HM with  $m_1(m_3) = 0.07(0.065)$  eV.



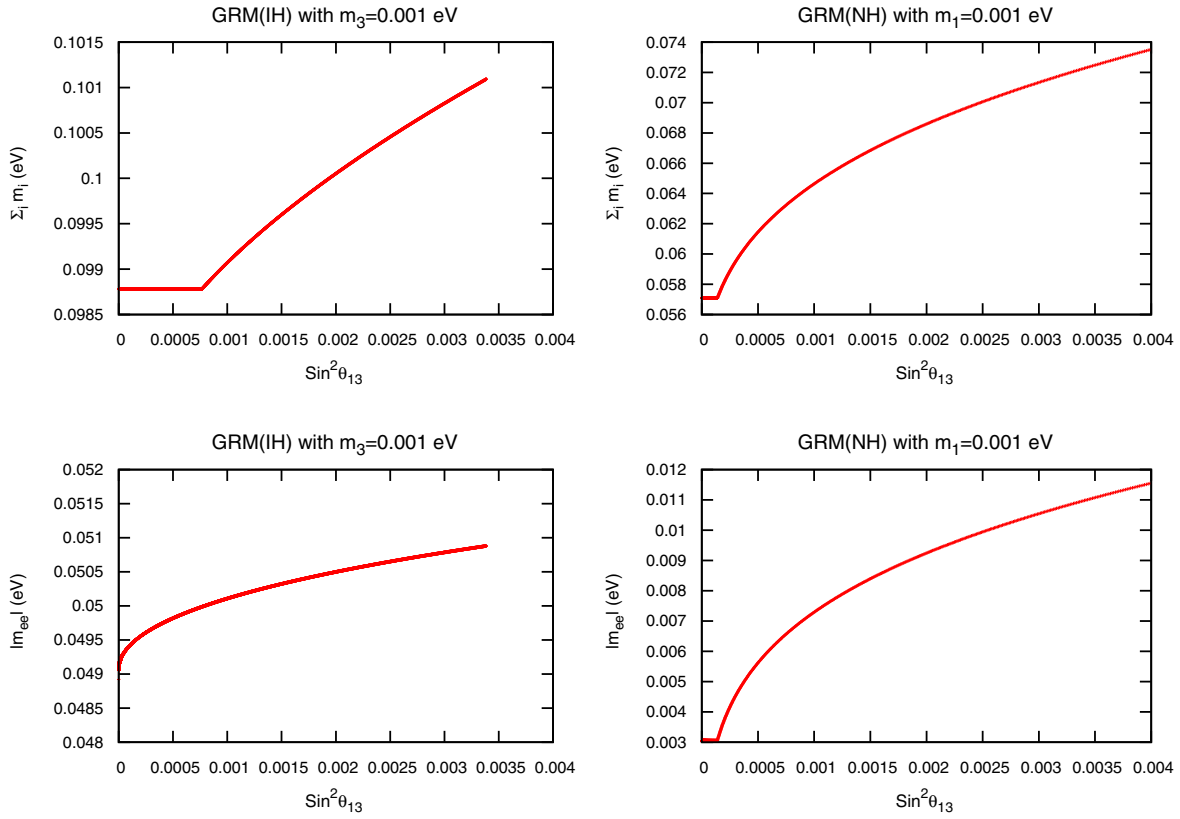


FIG. 31 (color online).  $\sum_i |m_i|$  and  $|m_{ee}|$  with  $\sin^2 \theta_{13}$  for GRM with  $m_1(m_3) = 0.001$  eV.

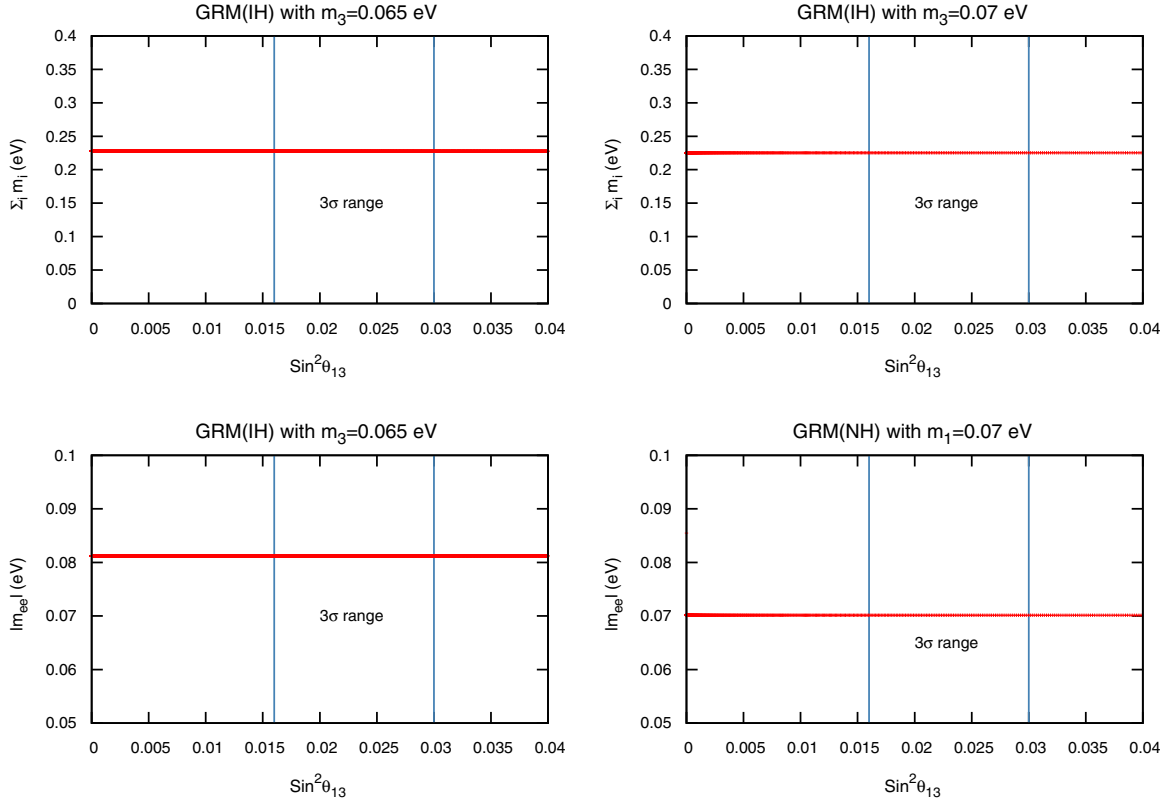


FIG. 32 (color online).  $\sum_i |m_i|$  and  $|m_{ee}|$  with  $\sin^2 \theta_{13}$  for GRM with  $m_1(m_3) = 0.07(0.065)$  eV.

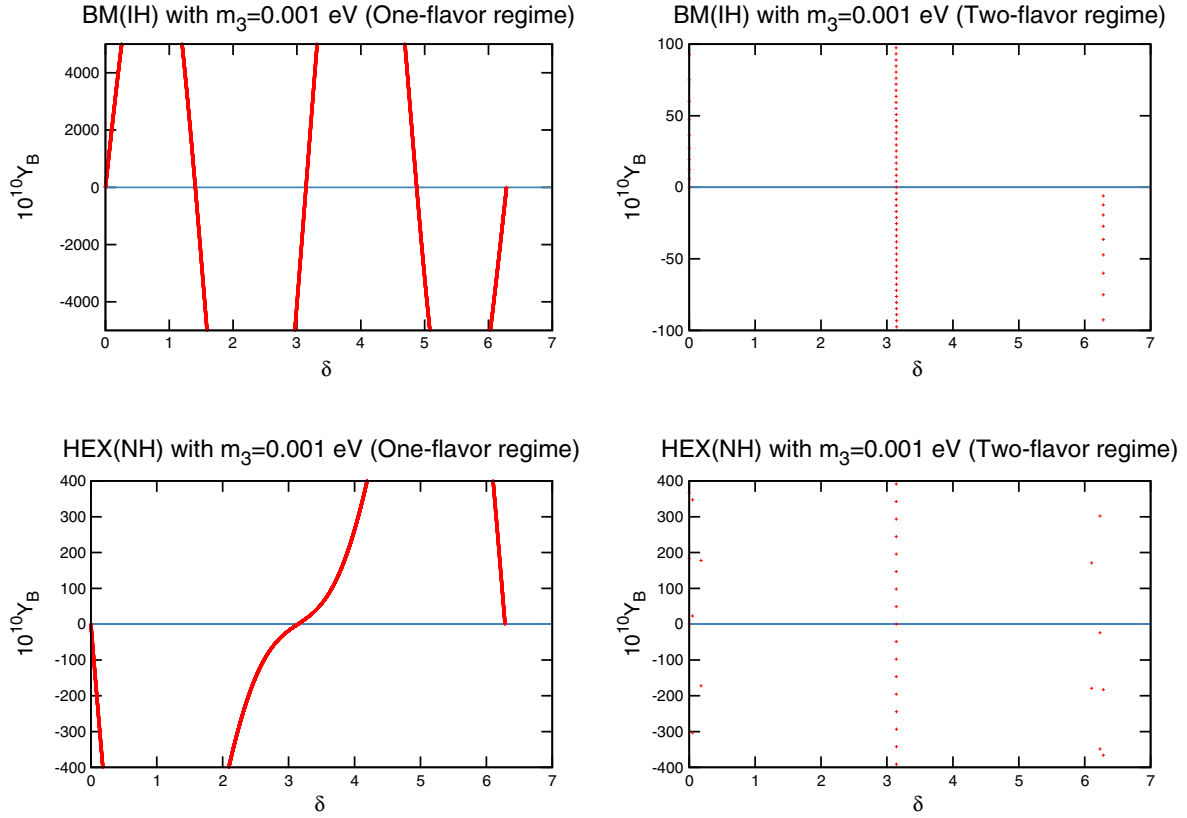


FIG. 33 (color online). Variation of baryon asymmetry with  $\delta$  for BM and HM.

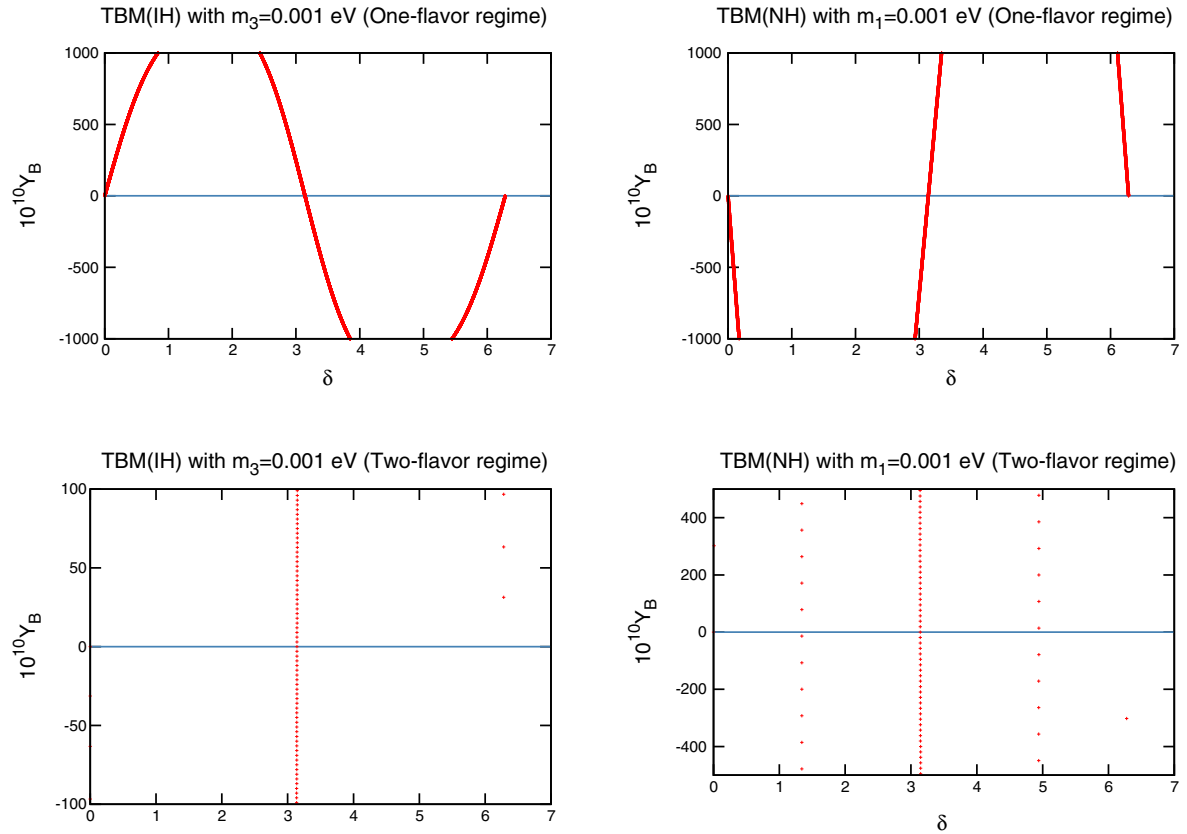


FIG. 34 (color online). Variation of baryon asymmetry with  $\delta$  for TBM.

TABLE VIII. Parameters used in the calculation of baryogenesis.

Parameters	TBM (IH)	TBM (NH)	BM (IH)	HEX (NH)
$w$	0.004435	0.004575	0.00461	0.00461
$\sin^2 \theta_{13}$	0.01621	0.01672	0.01622	0.01621
$\sin^2 \theta_{23}$	0.4105	0.5918	0.4102	0.5937

TABLE IX. Values of  $\delta$  giving rise to correct baryon asymmetry.

Model	$\delta$ for 1 flavor (rad)	$\delta$ for 2 flavor (in rad)
TBM (IH), $m_3 = 0.001$	0.00329867–0.0043982297, 3.1376656–3.13860814	3.14190681
TBM (NH), $m_1 = 0.001$	3.14269221–3.14300637, 6.282085749–6.282242829	...
BM (IH), $m_3 = 0.001$	0.000314159, 1.40711935, 4.8754376	0.0001570769
HEX (NH), $m_1 = 0.001$	3.182276–3.1981413, 6.28020079–6.2808291	...

TABLE X. Summary of results. The symbol  $\checkmark$  ( $\times$ ) is used when the particular parameter in the column can (cannot) be realized within a particular model denoted by the row.

Model	$\Delta m_{21}^2$	$\Delta m_{23}^2 \Delta m_{31}^2$	$\theta_{13}$	$\theta_{23}$	$\theta_{12}$	$\sum  m_i $	$Y_B(1 \text{ flavor})$	$Y_B(2 \text{ flavor})$	$Y_B(3 \text{ flavor})$
BM (IH) ( $m_3 = 0.001$ )	$\checkmark$	$\checkmark$	$\checkmark$	$\checkmark$	$\checkmark$	$\checkmark$	$\checkmark$	$\checkmark$	$\times$
BM (NH) ( $m_1 = 0.001$ )	$\checkmark$	$\checkmark$	$\checkmark$	$\checkmark$	$\times$	$\checkmark$	$\times$	$\times$	$\times$
BM (IH) ( $m_3 = 0.065$ )	$\times$	$\checkmark$	$\checkmark$	$\checkmark$	$\times$	$\checkmark$	$\times$	$\times$	$\times$
BM (NH) ( $m_1 = 0.07$ )	$\checkmark$	$\checkmark$	$\checkmark$	$\checkmark$	$\times$	$\checkmark$	$\times$	$\times$	$\times$
TBM (IH) ( $m_3 = 0.001$ )	$\checkmark$	$\checkmark$	$\checkmark$	$\checkmark$	$\checkmark$	$\checkmark$	$\checkmark$	$\checkmark$	$\times$
TBM (NH) ( $m_1 = 0.001$ )	$\checkmark$	$\checkmark$	$\checkmark$	$\checkmark$	$\checkmark$	$\checkmark$	$\checkmark$	$\times$	$\times$
TBM (IH) ( $m_3 = 0.065$ )	$\times$	$\checkmark$	$\checkmark$	$\checkmark$	$\checkmark$	$\checkmark$	$\times$	$\times$	$\times$
TBM (NH) ( $m_1 = 0.07$ )	$\times$	$\checkmark$	$\checkmark$	$\checkmark$	$\checkmark$	$\checkmark$	$\times$	$\times$	$\times$
HM (IH) ( $m_3 = 0.001$ )	$\checkmark$	$\checkmark$	$\checkmark$	$\checkmark$	$\times$	$\checkmark$	$\times$	$\times$	$\times$
HM (NH) ( $m_1 = 0.001$ )	$\checkmark$	$\checkmark$	$\checkmark$	$\checkmark$	$\checkmark$	$\checkmark$	$\checkmark$	$\times$	$\times$
HM (IH) ( $m_3 = 0.065$ )	$\times$	$\checkmark$	$\checkmark$	$\checkmark$	$\checkmark$	$\checkmark$	$\times$	$\times$	$\times$
HM (NH) ( $m_1 = 0.07$ )	$\times$	$\checkmark$	$\checkmark$	$\checkmark$	$\checkmark$	$\checkmark$	$\times$	$\times$	$\times$
GRM (IH) ( $m_3 = 0.001$ )	$\times$	$\times$	$\times$	$\times$	$\times$	$\checkmark$	$\times$	$\times$	$\times$
GRM (NH) ( $m_1 = 0.001$ )	$\checkmark$	$\checkmark$	$\checkmark$	$\times$	$\times$	$\checkmark$	$\times$	$\times$	$\times$
GRM (IH) ( $m_3 = 0.065$ )	$\times$	$\times$	$\checkmark$	$\times$	$\times$	$\checkmark$	$\times$	$\times$	$\times$
GRM (NH) ( $m_1 = 0.07$ )	$\times$	$\times$	$\checkmark$	$\times$	$\times$	$\checkmark$	$\times$	$\times$	$\times$

value of the branching ratios are found to lie very close to the experimental limit. Both the prediction of the LFV process and origin of nonzero reactor mixing angle are consistent with allowed strength of the perturbation term  $\omega$  arising from the type II seesaw mechanism.

We summarize our results for all the models under consideration in Table X. We also show the preferred values of Dirac  $CP$  phase  $\delta$  for successful leptogenesis in Table IX. More precise experimental data from neutrino oscillation and cosmology experiments should be able to falsify or verify some of the models discussed in this work.

### ACKNOWLEDGMENTS

S. Patra and M. K. Das would like to thank the organizers of the Workshop on High Energy Physics and Phenomenology (WHEPP13), held at Puri, Odisha, India, December 12–21, 2013, where the idea was proposed. The work of S. Patra is supported by the Department of Science and Technology, Government of India, under the financial Grant No. SB/S2/HEP-011/2013. The work of M. K. Das is partially supported by Grant No. 42-790/2013 (SR) from University Grants Commission, Government of India.

- [1] S. Fukuda *et al.* (Super-Kamiokande Collaboration), *Phys. Rev. Lett.* **86**, 5656 (2001); Q. R. Ahmad *et al.* (SNO Collaboration), *Phys. Rev. Lett.* **89**, 011301 (2002); **89**, 011302 (2002); J. N. Bahcall and C. Pena-Garay, *New J. Phys.* **6**, 63 (2004); K. Nakamura *et al.*, *J. Phys. G* **37**, 075021 (2010).
- [2] K. Abe *et al.* (T2K Collaboration), *Phys. Rev. Lett.* **107**, 041801 (2011).
- [3] Y. Abe *et al.*, *Phys. Rev. Lett.* **108**, 131801 (2012).
- [4] F. P. An *et al.* (DAYA-BAY Collaboration), *Phys. Rev. Lett.* **108**, 171803 (2012).
- [5] J. K. Ahn *et al.* (RENO Collaboration), *Phys. Rev. Lett.* **108**, 191802 (2012).
- [6] M. C. Gonzalez-Garcia, M. Maltoni, J. Salvado, and T. Schwetz, *J. High Energy Phys.* **12** (2012) 123.
- [7] G. L. Fogli, E. Lisi, A. Marrone, D. Montanino, A. Palazzo, and A. M. Rotunno, *Phys. Rev. D* **86**, 013012 (2012).
- [8] P. Minkowski, *Phys. Lett.* **67B**, 421 (1977); M. Gell-Mann, P. Ramond, and R. Slansky, (CERN) print-80-0576 1980; T. Yanagida, in *Proceedings of the Workshop on the Baryon Number of the Universe and Unified Theories, Tsukuba, Japan, 1979* (unpublished); R. N. Mohapatra and G. Senjanovic, *Phys. Rev. Lett.* **44**, 912 (1980); J. Schechter and J. W. F. Valle, *Phys. Rev. D* **22**, 2227 (1980).
- [9] R. N. Mohapatra and G. Senjanovic, *Phys. Rev. D* **23**, 165 (1981); G. Lazarides, Q. Shafi and C. Wetterich, *Nucl. Phys.* **B181**, 287 (1981); C. Wetterich, *Nucl. Phys.* **B187**, 343 (1981); B. Brahmachari and R. N. Mohapatra, *Phys. Rev. D* **58**, 015001 (1998); R. N. Mohapatra, *Nucl. Phys. B, Proc. Suppl.* **138**, 257 (2005); S. Antusch and S. F. King, *Phys. Lett. B* **597**, 199 (2004).
- [10] R. Foot, H. Lew, X. G. He, and G. C. Joshi, *Z. Phys. C* **44**, 441 (1989).
- [11] F. Vissani, arXiv:hep-ph/9708483; V. D. Barger, S. Pakvasa, T. J. Weiler, and K. Whisnant, *Phys. Lett. B* **437**, 107 (1998); A. J. Baltz, A. S. Goldhaber, and M. Goldhaber, *Phys. Rev. Lett.* **81**, 5730 (1998).
- [12] P. F. Harrison, D. H. Perkins, and W. G. Scott, *Phys. Lett. B* **530**, 167 (2002); P. F. Harrison and W. G. Scott, *Phys. Lett. B* **535**, 163 (2002); Z. z. Xing, *Phys. Lett. B* **533**, 85 (2002); P. F. Harrison and W. G. Scott, *Phys. Lett. B* **547**, 219 (2002); **557**, 76 (2003); **594**, 324 (2004).
- [13] C. H. Albright, A. Dueck, and W. Rodejohann, *Eur. Phys. J. C* **70**, 1099 (2010).
- [14] A. Datta, F.-S. Ling, and P. Ramond, *Nucl. Phys.* **B671**, 383 (2003); Y. Kajiyama, M. Raidal, and A. Strumia, *Phys. Rev. D* **76**, 117301 (2007); L. L. Everett and A. J. Stuart, *Phys. Rev. D* **79**, 085005 (2009); F. Feruglio and A. Paris, *J. High Energy Phys.* **03** (2011) 101; G.-J. Ding, L. L. Everett, and A. J. Stuart, *Nucl. Phys.* **B857**, 219 (2012); I. K. Cooper, S. F. King, and A. J. Stuart, *Nucl. Phys.* **B875**, 650 (2013).
- [15] Y. Shimizu, M. Tanimoto, and A. Watanabe, *Prog. Theor. Phys.* **126**, 81 (2011); S. F. King and C. Luhn, *J. High Energy Phys.* **09** (2011) 042; S. Antusch, S. F. King, C. Luhn, and M. Spinrath, *Nucl. Phys.* **B856**, 328 (2012); S. F. King and C. Luhn, *J. High Energy Phys.* **03** (2012) 036; S. Gupta, A. S. Joshipura, and K. M. Patel, *Phys. Rev. D* **85**, 031903 (2012); S.-F. Ge, D. A. Dicus, and W. W. Repko, *Phys. Rev. Lett.* **108**, 041801 (2012); S.-F. Ge, H.-J. He, and F.-R. Yin, *J. Cosmol. Astropart. Phys.* **05** (2010) 017; S.-F. Ge, D. A. Dicus, and W. W. Repko, *Phys. Lett. B* **702**, 220 (2011); M.-C. Chen, J. Huang, J.-M. O'Bryan, A. M. Wijangco, and F. Yu, *J. High Energy Phys.* **02** (2013) 021; J. Liao, D. Marfatia, and K. Whisnant, *Phys. Rev. D* **87**, 013003 (2013); B. Karmakar and A. Sil, arXiv:1407.5826; H.-J. He and F.-R. Yin, *Phys. Rev. D* **84**, 033009 (2011); H.-J. He and X.-J. Xu, *Phys. Rev. D* **86**, 111301 (2012).
- [16] G. Altarelli, F. Feruglio, L. Merlo, and E. Stamou, *J. High Energy Phys.* **08** (2012) 021.
- [17] P. A. R. Ade *et al.* (Planck Collaboration), arXiv:1303.5076.
- [18] V. A. Kuzmin, V. A. Rubakov, and M. E. Shaposhnikov, *Phys. Lett.* **155B**, 36 (1985).
- [19] M. Fukugita and T. Yanagida, *Phys. Lett. B* **174**, 45 (1986).
- [20] J. Ellis, S. Lola, and D. V. Nanopoulos, *Phys. Lett. B* **452**, 87 (1999); G. Lazarides and N. D. Vlachos, *Phys. Lett. B* **459**, 482 (1999); M. S. Berger and B. Brahmachari, *Phys. Rev. D* **60**, 073009 (1999); M. S. Berger, *Phys. Rev. D* **62**, 013007 (2000); W. Buchmüller and M. Plumacher, *Int. J. Mod. Phys. A* **15**, 5047 (2000); K. Kang, S. K. Kang, and U. Sarkar, *Phys. Lett. B* **486**, 391 (2000); H. Goldberg, *Phys. Lett. B* **474**, 389 (2000); R. Jeannerot, S. Khalil, and G. Lazarides, *Phys. Lett. B* **506**, 344 (2001); D. Falcone and F. Tramontano, *Phys. Rev. D* **63**, 073007 (2001); *Phys. Lett. B* **506**, 1 (2001); H. B. Nielsen and Y. Takanishi, *Phys. Lett. B* **507**, 241 (2001); E. Nezri and J. Orloff, *J. High Energy Phys.* **04** (2003) 020.
- [21] A. S. Joshipura, E. A. Paschos, and W. Rodejohann, *Nucl. Phys.* **B611**, 227 (2001).
- [22] S. Davidson, E. Nardi, and Y. Nir, *Phys. Rep.* **466**, 105 (2008).
- [23] D. Borah and M. K. Das, *Phys. Rev. D* **90**, 015006 (2014).
- [24] D. Borah, *Nucl. Phys.* **B876**, 575 (2013); D. Borah, S. Patra, and P. Pritimita, *Nucl. Phys.* **B881**, 444 (2014).
- [25] D. Borah, *Int. J. Mod. Phys. A* **29**, 1450108 (2014).
- [26] W. Rodejohann, *Phys. Rev. D* **70**, 073010 (2004); M. Lindner and W. Rodejohann, *J. High Energy Phys.* **05** (2007) 089; D. A. Sierra, I. de M. Varzielas and E. Houet, *Phys. Rev. D* **87**, 093009 (2013); D. A. Sierra and I. de Medeiros Varzielas, *J. High Energy Phys.* **07** (2014) 042.
- [27] M. K. Das, D. Borah, and R. Mishra, *Phys. Rev. D* **86**, 095006 (2012); D. Borah and M. K. Das, *Nucl. Phys.* **B870**, 461 (2013).
- [28] D. Borah, *Phys. Rev. D* **87**, 095009 (2013).
- [29] S. Weinberg, *Phys. Rev. Lett.* **43**, 1566 (1979).
- [30] H. Ishimori, T. Kobayashi, H. Ohki, Y. Shimizu, H. Okada, and M. Tanimoto, *Prog. Theor. Phys. Suppl.* **183**, 1 (2010); W. Grimus and P. O. Ludl, *J. Phys. A* **45**, 233001 (2012); S. F. King and C. Luhn, *Rep. Prog. Phys.* **76**, 056201 (2013); G. Altarelli and F. Feruglio, *Nucl. Phys.* **B741**, 215 (2006); E. Ma and D. Wegman, *Phys. Rev. Lett.* **107**, 061803 (2011); S. Gupta, A. S. Joshipura, and K. M. Patel, *Phys. Rev. D* **85**, 031903 (2012); S. Dev, R. R. Gautam, and L. Singh, *Phys. Lett. B* **708**, 284 (2012); P.-H. Gu and H.-J. He, *J. Cosmol. Astropart. Phys.* **12** (2006) 010; *Phys. Rev. D* **86**, 111301 (2012); G. C. Branco, R. Gonzalez Felipe, F. R. Joaquim, and H. Serodio, *Phys. Rev. D* **86**, 076008 (2012); E. Ma, *Phys. Lett. B* **660**, 505 (2008); F. Plentinger, G. Seidl, and W. Winter, *J. High Energy Phys.* **04** (2008) 077; N. Haba, R. Takahashi, M. Tanimoto, and K. Yoshioka,

- Phys. Rev. D* **78**, 113002 (2008); S.-F. Ge, D. A. Dicus, and W. W. Repko, *Phys. Rev. Lett.* **108**, 041801 (2012); E. Ma and R. Rajasekaran, *Phys. Rev. D* **64**, 113012 (2001); E. Ma, in VI-Silafac, Puerto Vallarta, Mexico, Nov. 2006 (unpublished), [arXiv:gr-qc/0612013](https://arxiv.org/abs/gr-qc/0612013)*Phys. Rev. D* **70**, 031901 (2004); T. Araki and Y.F. Li, *Phys. Rev. D* **85**, 065016 (2012); Z.-z. Xing, *Chin. Phys. C* **36**, 281 (2012); *Phys. Lett. B* **696**, 232 (2011); P. S. Bhupal Dev, B. Dutta, R. N. Mohapatra, and M. Severson, *Phys. Rev. D* **86**, 035002 (2012); B. Adhikary, B. Brahmachari, A. Ghosal, E. Ma, and M. K. Parida, *Phys. Lett. B* **638**, 345 (2006); G. Altarelli and F. Feruglio, *Rev. Mod. Phys.* **82**, 2701 (2010); K. M. Parattu and A. Wingerter, *Phys. Rev. D* **84**, 013011 (2011); R. Gonzalez Felipe, H. Serodio, and J. P. Silva *Phys. Rev. D* **88**, 015015 (2013).
- [31] E. W. Kolb and M. S. Turner, *The Early Universe, Frontiers in Physics* (Addison-Wesley, Redwood, CA, 1990), Vol. 69; A. Pilaftsis, *Int. J. Mod. Phys. A* **14**, 1811 (1999); E. A. Paschos and M. Flanz, *Phys. Rev. D* **58**, 113009 (1998).
- [32] R. Barbieri, P. Creminelli, A. Strumia, and N. Tetradis, *Nucl. Phys.* **B575**, 61 (2000); A. Abada, S. Davidson, F.-X. Josse-Michaux, M. Losada, and A. Riotto, *J. Cosmol. Astropart. Phys.* **04** (2006) 004; E. Nardi, Y. Nir, E. Roulet, and J. Racker, *J. High Energy Phys.* **01** (2006) 164; A. Abada, S. Davidson, A. Ibarra, F.-X. Josse-Michaux, M. Losada, and A. Riotto, *J. High Energy Phys.* **09** (2006) 010.
- [33] G. Lazarides and Q. Shafi, *Phys. Rev. D* **58**, 071702 (1998); T. Hambye and G. Senjanovic, *Phys. Lett. B* **582**, 73 (2004).
- [34] J. Adam *et al.* (MEG Collaboration), *Phys. Rev. Lett.* **107**, 171801 (2011).
- [35] P. Fileviez Perez, T. Han, and T. Li, *Phys. Rev. D* **80**, 073015 (2009); D. Aristizabal Sierra, M. Hirsch, J. Valle, and A. Villanova del Moral, *Phys. Rev. D* **68**, 033006 (2003); S. M. Boucenna, S. Morisi, and J. W. F. Valle, *Adv. High Energy Phys.* **2014**, 1 (2014).
- [36] P. Fileviez Perez, T. Han, G.-y. Huang, T. Li, and K. Wang, *Phys. Rev. D* **78**, 015018 (2008).
- [37] A. Baldini *et al.*, MEG Upgrade Proposal, [arXiv:1301.7225](https://arxiv.org/abs/1301.7225).
- [38] U. Bellgardt *et al.* (SINDRUM Collaboration), *Nucl. Phys.* **B299**, 1 (1988).
- [39] A. Blondel *et al.*, [arXiv:1301.6113](https://arxiv.org/abs/1301.6113).